

**Sequence Stratigraphy Analysis and Facies  
Modeling of Submarine Fan Reservoir, Pari Field,  
Kutai Basin, Offshore East Kalimantan, Indonesia**

**Thesis**

By:

Roy Rahadi

0606001475



University of Indonesia  
Faculty of Mathematics and Natural Sciences  
Physics Graduate Program  
Reservoir Geophysics Section  
2009

**Sequence Stratigraphy Analysis and Facies  
Modeling of Submarine Fan Reservoir, Pari Field,  
Kutai Basin, Offshore East Kalimantan, Indonesia**

**Thesis**

Submitted in Partial Fulfillment of the Requirements for the Degree of  
Master of Science in Reservoir Geophysics

By:

Roy Rahadi

0606001475



University of Indonesia  
Faculty of Mathematics and Natural Sciences  
Physics Graduate Program  
Reservoir Geophysics Section  
2009

## Approval Page

Thesis title : Sequence Stratigraphy Analysis and Facies Modeling of  
Submarine Fan Reservoir, Pari Field, Kutai Basin,  
Offshore East Kalimantan, Indonesia  
Author : Roy Rahadi  
Student number : 0606001475

Has been approved by the committee members:

**Dr. Abdul Haris**  
Supervisor

**Prof. Dr. Suprajitno Munadi**  
Examiner

**Dr. Carlos Tarazona**  
Examiner

**Dr. Ricky A. Wibowo**  
Examiner

University of Indonesia  
Faculty of Mathematics and Natural Sciences  
Physics Graduate Program  
Reservoir Geophysics Section  
Chairman,

**Dr. Dedi Suyanto**  
NIP. 130 935 271

Defense date: 20 March 2009

## Acknowledgements

I extend sincere gratitude and deepest appreciation to my thesis committee members for their support and time to helping me to pursue my master degree in reservoir geophysics. I especially thanks to Dr. Abdul Haris for serving as my supervisor on this project. I am thankful to the staff of the Reservoir Geophysics Department at the University of Indonesia who has been wonderful in supporting me.

I would like to express my thanks to Chevron Indonesia Company for permission using the data for this thesis project. My gratitude is extended to Kevin Kveton (Chevron Indonesia Exploration & New Venture Manager), Mirzal Nur Ardhie, Befriko Saparindra Murdianto and to all staff members at Chevron Indonesia Company for their assistance during the work and for sharing their extensive knowledge.

Special thanks go to my parents and families for their love and support, to encourage me for the success of my study. I would dedicate this to my special persons in my life, my wife, Laurensia Hartina and my son, Kenzie Nicolay Rahadi, only because of their love and happiness; I can keep strong and became a better person through days.

What I am most grateful for that all of those mentioned above, as well as many others not mentioned here, were willing to help, encourage, and support me. I am thankful to that. To them I am indebted greatly and forever. Thank you one and all.

Jakarta, February 2009

Author

## Abstract

Seismic sequence stratigraphy analysis was performed to identify a chronostratigraphic evolution of submarine fan reservoir in Pari field, Makassar Strait, offshore East Kalimantan. A complete sequence stratigraphy in Pari field was divided into three systems tract: lowstand systems tract (LST), transgressive systems tract (TST) and highstand systems tract (HST). The "X" reservoir unit was deposited during the lowstand systems tract (LST). Based on core data and well log, the reservoir is dominated by few massive thick sandstone, thin interbedded sandstone and shale. Well data and 3D seismic multiattribute analysis indicated a submarine fan depositional system feature. However, the available 3D seismic data could not image the submarine fan elements feature like channels and splay lobes due to low seismic resolution. A shallow Pleistocene submarine fan located in the northern part of the study area is clearly imaged using 3D seismic data. That Pleistocene submarine fan provides analog dimensions for sub-seismic reservoir elements in the "X" reservoir unit, Pari field. The dimensions of channels and splay lobes within Pleistocene submarine fan were used to define stochastically reservoir elements in Pari field. The Pleistocene submarine fan are approximately the same size as the seismically mapped the "X" reservoir unit. Three facies model were generated to provide multiple realizations of facies model. Those are 70% channel and 30% splay lobe (more channels dominated), 50% channel and 50% splay lobe (proportional between channel and splay lobe), and 30% channel and 70% splay lobe (more splay lobe dominated).

## Table of Contents

Title Page.....	i
Approval Page .....	ii
Acknowledgements.....	iii
Abstract.....	iv
Table of Contents .....	v
List of Figures .....	vii
List of Tables.....	xi
List of Tables.....	xi
Chapter 1 .....	1
Introduction .....	1
1.1 Thesis Objective .....	2
1.2 Problem limitation .....	3
1.3 Thesis Structure .....	3
1.4 Available Datasets .....	4
1.5 Software and Hardware used .....	4
Chapter 2 .....	5
Geological Setting and Sequence Stratigraphy Concept.....	5
2.1 Pari Field Geography .....	5
2.2 Pari Field Geological Setting .....	6
2.3 Pari Field Stratigraphy .....	8
2.4 Seismic Sequence Stratigraphy Concept .....	9
2.5 Models for Submarine Fan Deposition within a Sequence Stratigraphic Framework.....	12
2.5.1 Lowstand Fan.....	14
2.5.2 Lowstand Wedge.....	16
2.6 Element of Submarine Fan Systems .....	17
Chapter 3 .....	23
Geostatistical Integration of Well and Seismic Data.....	23
3.1 Introduction .....	23
3.2 Reservoir Facies Modeling .....	24
3.2.1 Seismic Multiattribute Method .....	24
3.2.2 Object Based Modeling Method .....	27
3.2.3 Variogram – a measure of spatial variability .....	27
Chapter 4 .....	32
Application to Real Datasets: a Cased Study of Pari field, Kutai Basin, Offshore East Kalimantan, Indonesia.....	32
4.1 Core Data Analysis .....	32
4.1.1 Core Description from Pari-2 Well.....	33
4.1.2 Core Description from Pari-5 Well.....	38
4.2 Sequence Stratigraphy Framework of Pari Field.....	42
4.3 Pari Field Structural Modeling.....	52
4.4 Pari Field Facies Modeling.....	54
4.4.1 Well Data Analysis .....	54
4.4.2 Seismic Multiattribute Analysis.....	59
4.4.3 Object Based Facies Modeling .....	64
4.4.4 Submarine Fan Analogue.....	65

4.4.5 Pari Field Facies Modeling Result.....	70
Chapter 5 .....	73
Conclusions and Recommendations .....	73
5.1 Conclusions.....	73
5.2 Recommendations for future work.....	74
References.....	75



## List of Figures

Figure 2.1 Pari Field is located in the Makassar Strait, southern Mahakam Delta, offshore East Kalimantan (picture taken from goggle earth website).....	5
Figure 2.2 Geological setting of Kutai Basin with distribution of hydrocarbon fields (adapted from Mamuaya et al., 1995).....	7
Figure 2.3 Tectonostratigraphy of Kutai Basin, blue box showing relative stratigraphic position of the objective reservoir (adapted from Moss et al., 1999).....	9
Figure 2.4 Diagram showing reflection termination patterns and type of discontinuities (adapted from Mitchum and Vail, 1977).....	11
Figure 2.5 Type of seismic reflection pattern and configuration within sequences (adapted from Mitchum and Vail, 1977).....	12
Figure 2.6 Conceptual block diagrams of the lowstand system tract: (A) lowstand fan, (B) early lowstand wedge (channel-levee complex), (C) late lowstand wedge (prograding complex), and (D) an axial section through the canyon and slope (adapted from Posamentier and Vail, 1985, 1988).....	14
Figure 2.7 Relative sea levels as a function of eustacy and total subsidence (thermal cooling, tectonics, sediment loading and compaction). .....	15
Figure 2.8 Characteristics of lowstand fan and lowstand wedge time (adapted from Posamentier and Vail, 1985, 1988).....	17
Figure 2.9 Main types of channel-fill deposits observed in ancient turbidites. Vertical scale ranges from several meters to tens of meters and horizontal scale ranges from tens of meters to hundreds of meters .....	19
Figure 2.10 Physiographic map of submarine fan showing (A) levee, (B) distal overbank, (C) large scale scours, (D) channel floor, and (E) depositional lobes (adapted from Normark et al., 1980). .....	20
Figure 2.11 Main characteristic features of channel, channel-lobe transition, and lobe deposits (adapted from Mutti and Normark, 1987).....	22
Figure 2.12 Geomorphic elements, depositional unit Isopach, and log responses of a channel-lobe complex (adapted from Galloway, W.E., and D.K. Hobday, 1996). .....	22
Figure 3.1 Assuming the case of three seismic attributes, each target log sample is modeled as a linear combination of attribute samples at the same time. ....	25
Figure 3.2 Applying nonlinear transforms to both the target and the attribute data improves the correlation between the two.....	26
Figure 3.3 Applying the multiattribute transform using six attributes and a seven-point operator. Only the first three wells are shown. The original porosity log is shown in black; the predicted log is shown in	



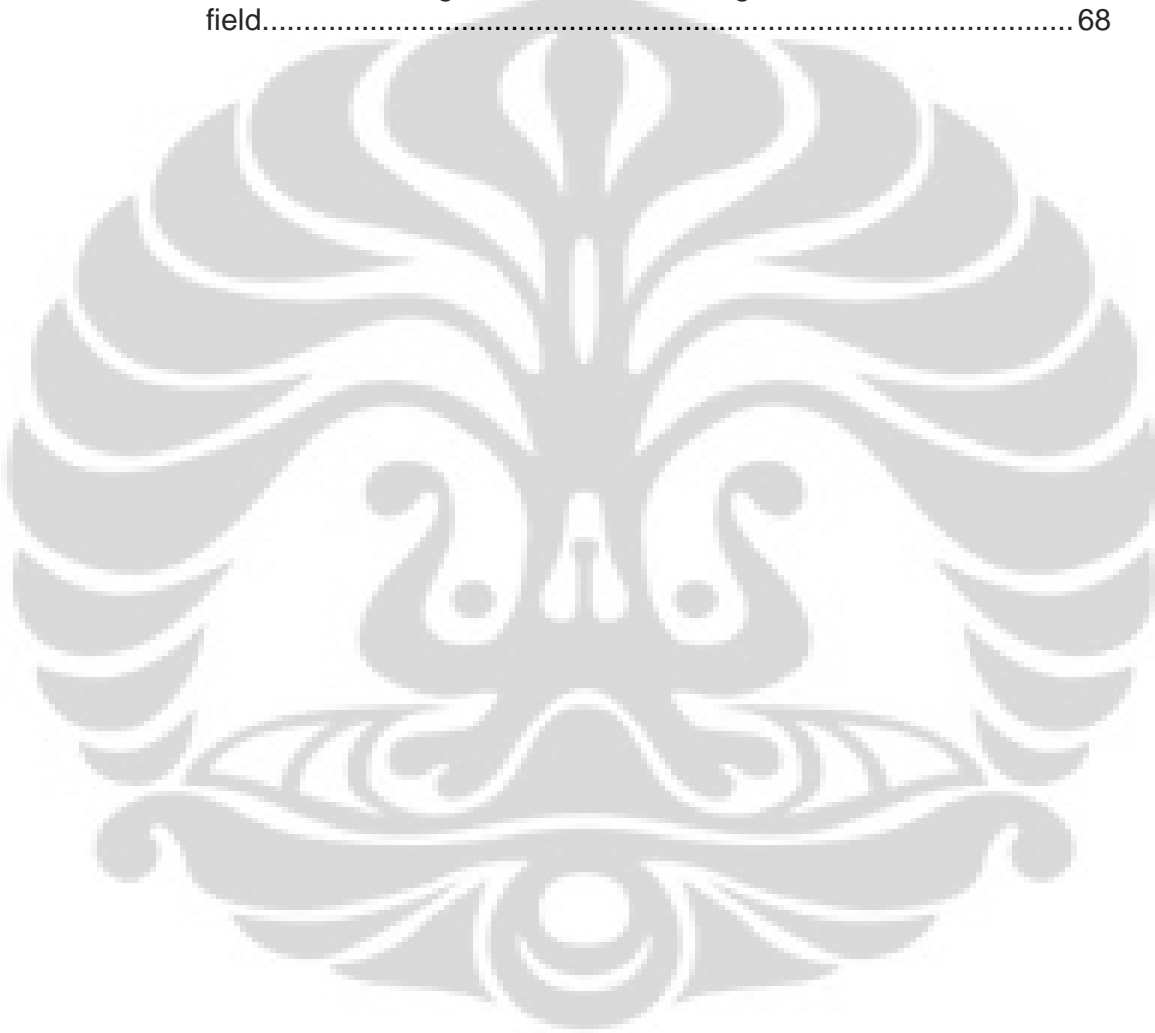
red. The normalized correlation coefficient for all the wells is 0.69. .....	26
Figure 3.4 Parts of a variogram. The nugget quantifies measurement inconsistency and the range is the break point between correlated and uncorrelated data. ....	30
Figure 3.5 Facies determination can be simplified into two main categories: deterministic and stochastic method.....	30
Figure 3.6 Thesis work flow .....	31
Figure 4.1 Representative log response and core photograph from Pari-2 Well. The core photograph illustrates the gray shale with coral fragments. ....	34
Figure 4.2 Representative log response and core photograph from Pari-2 Well. The core photograph illustrates vertical burrow on near top of sandstone overlain with gray shale. ....	35
Figure 4.3 Representative log response and core photograph from Pari-2 Well. The core photograph illustrates interbedded light brown sandstone with gray shale with organic material and rippled cross stratification.....	35
Figure 4.4 Representative log response and core photograph from Pari-2 Well. The core photograph illustrates massive sandstone with shale clast conglomerates.....	36
Figure 4.5 Representative log response and core photograph from Pari-2 Well. The core photograph illustrates burrowed and rippled sand in shale.....	37
Figure 4.6 Representative log response and core photograph from Pari-2 Well. The core photograph illustrates light brown sand with massive structure in lower part, horizontal lamination and rippled structure. ....	38
Figure 4.7 Representative log response and core photograph from Pari-5 Well. The core photograph illustrates bioturbated shale has a burrowed contact with the underlying unit (shale with thin sand beds). ....	39
Figure 4.8 Representative log response and core photograph from Pari-5 Well. The core photograph illustrates interbedded light brown sand and gray shale with burrows structure.....	40
Figure 4.9 Representative log response and core photograph from Pari-5 Well. The core photograph illustrates light brown fine grained sand with dark gray shale. Laminated structure in sand is mainly fossil leaves.....	41
Figure 4.10 Interpreted depositional facies in general based on conventional core data in Pari-2 and Pari-5 wells within "X" reservoir unit. ....	42
Figure 4.11 Type log in Pari-5 well illustrates the well log expression of the systems tract and seismic reflection display across Pari-5 well. The systems tract consists of lowstand systems tract (LST), transgressive systems tract (TST) and highstand systems tract	

(HST) with each systems tract shows specific well log expression and seismic reflection. ....	45
Figure 4.12 Interpreted seismic section northwest-southeast direction along submarine fan systems across Pari-5, Pari-1 and Pari-3 wells. ....	46
Figure 4.13 Interpreted seismic section north-south direction crossing the submarine fan systems across Pari-2 and Pari-1 wells.....	47
Figure 4.14 Interpreted seismic section southwest-northeast direction crossing the submarine fan systems across Pari-5 well.....	47
Figure 4.15 Interpreted seismic section southwest-northeast direction in the proximal part of submarine fan systems.....	48
Figure 4.17 Interpreted depth structure map on each sequence boundary over the study area (A) Top structure map on upper highstand systems tract (B) Top structure map on transgressive systems tract (C) Top structure map on lowstand systems tract (D) Top structure map on lower highstand systems tract (E) 3D view of the depth structure maps. ....	50
Figure 4.18 Three Dimensional (3D) view showing seismic intersection and interpreted sequence boundary of submarine fan.....	51
Figure 4.19 Isopach map of "X" reservoir unit showed the outer limit of submarine fan gross sands and relative sediment source from northwest direction.....	51
Figure 4.20 Seismic amplitude display (above) and seismic attribute coherency display (below). The seismic display indicated no obvious fault developed in Pari field. Seismic amplitude discontinuity appears to indicate small fault which consider has no significant effect in reservoir modeling. ....	53
Figure 4.21 Three dimensional (3D) model showing the structural framework and layering of the main reservoir interval in the Pari field.....	53
Figure 4.22 Correlation from Pari-5 to Pari-2 wells within "X" reservoir unit showing the log data (gamma ray, neutron-density) and interpreted lithofacies based on the net to gross cut-off and the final upscaled net to gross log. ....	56
Figure 4.23 Correlation from Pari-1 to Pari-3 wells within "X" reservoir unit showing the log data (gamma ray, neutron-density) and interpreted lithofacies based on the net to gross cut-off and the final upscaled net to gross log. ....	57
Figure 4.24 Thickness distribution for each lithofacies from Sequence Boundary (S.B) to Top of "X" reservoir unit. The dominant thickness is between 0 to 10 feet.....	58
Figure 4.25 The histogram plot showing the percentage of each lithofacies for the original well logs data compare with the upscaled cells from Sequence boundary (S.B) to Top of "X" reservoir unit. ....	58
Figure 4.27 Final attribute analysis showing the training error and validation error for each attribute with gamma ray log as the target log. ....	60

Figure 4.28 Cross plot between numbers of attributes versus average error from multiattribute analysis. ....	60
Figure 4.29 Cross plot between actual gamma ray versus predicted gamma ray using 7 attributes from all Pari wells. The cross plot showing 0.46 cross correlation. ....	61
Figure 4.31 Seismic amplitude maps (A) and seismic multiattribute maps (B) indicate gross submarine fan deposited used as a reservoir boundary for object based modeling, detail internal submarine fan configuration can not be resolved due to seismic resolution.....	63
Figure 4.32 Three dimensional (3D) view showing the seismic multiattribute overlaying with structural contour of top reservoir. Pari field is a large anticline with the submarine fan reservoir drape over the structure. ....	64
Figure 4.33 Map showing the study area and the Pleistocene submarine fan location in the northern part, offshore East Kalimantan, Indonesia. ....	67
Figure 4.34 Interpreted isochore map from 3D shallow seismic data shows mappable lobes configuration. The boundary area of the submarine fan shows with solid black line (Saller et al., 2004). ....	67
Figure 4.35 Seismic section display along Pleistocene submarine fan with detail interpretation of channel and lobe associated ((Saller et al., 2004). ....	69
Figure 4.36 Facies realization in the “X” reservoir unit with facies proportion 70% channel and 30% splay lobe (more channels dominated). ....	71
Figure 4.37 Facies realization in the “X” reservoir unit with facies proportion 50% channel and 50% splay lobe (proportional between channel and splay lobe). ....	71
Figure 4.38 Facies realization in the “X” reservoir unit with facies proportion 30% channel and 70% splay lobe (more splay lobes dominated). ....	72

## List of Tables

Table 4.1 Interpreted depth and gross thickness calculation for each sequence stratigraphic boundary in Pari wells. ....	55
Table 4.2 Geometry of splay lobe elements from Pleistocene submarine fan, used as an analogue for facies modeling in “X” reservoir unit in Pari field. ....	68
Table 4.3 Geometry of channel elements from Pleistocene submarine fan, used as an analogue for facies modeling in “X” reservoir unit in Pari field.....	68



# Chapter 1

## Introduction

The geologic community understands of submarine fans reservoir has grown considerably during the past two decade because it's became the major petroleum reservoirs in many sedimentary basins worldwide including basins in Indonesia. The reservoir prediction in submarine fans environment involves creating the spatial distribution of the reservoir properties by integration many different data. The data come from various sources and scales: from geological conceptual information in gigascope scale (in the order of kilometers), seismic data, well testing and log data in megascope scale (in the order of meters), to core data in macroscopic scale (in the order of centimeters). Integration of all data to generate a relatively unique reservoir description is challenging and technically difficult. In general, reservoir description can be briefly classified into two categories: the static properties description, which includes spatial descriptions of facies, porosity, permeability, and other properties; and dynamic description, which includes the variation in physical properties such as saturation, pressure as a function of time. Static description is critical in capturing the dynamic description. Typically, static properties such as facies and porosity can be reflected by core, log, and seismic data.

Statistically, seismic attributes such as the amplitude of the seismic data, can be used to estimate reservoir properties by integrating the spatial relationship of the seismic and the well data. However, this procedure does not always work well, especially when the spatial relationship of the reservoir properties is difficult to obtain, such as in the presence of a small number of wells. In this case, seismic information becomes important. The knowledge about the reservoir properties by integration of seismic data

should result in a better drilling decision and reduce the exploration risk. In addition, seismic data can also be used during the exploitation stage by integrating it with other dynamic information. This would help us better prediction the future performance of the reservoir.

## 1.1 Thesis Objective

Geological quantification is a topic that has always raised much interest and debate among geologists. Depending on the depositional environment a geologist is dealing with, and using the well data as a constraint, the geologist can draw sketches the distribution of the reservoirs. Unfortunately, hand-drawn cross sections are limited in the sense that they do not lead to a 3D model, and they represent only one possible model among infinity of scenarios matching the wells and compatible with the depositional environment. In general, well data are too sparsely distributed to predict lateral lithologic variations accurately. On the other hand, three-dimensional (3D) seismic data, with their dense lateral coverage, provide a valuable source of information for constraining earth models. With the increasing availability of high quality 3D seismic data and powerful workstations, there is now considerable interest in the utilization of seismic data to help improve the mapping of reservoir properties between wells.

With the high resolution 3D seismic data, wireline log and core data available in the study area, the objectives of this thesis work are to established sequence stratigraphy framework in Pari field and to build 3D static facies model in the main reservoir unit that capture all of the correctly scaled reservoir characteristics that have been identified from core data, well data and seismic data.

## **1.2 Problem limitation**

Sequence stratigraphy is the fundamental genetic stratigraphic units of the terrigenous basin fills. Each sequence stratigraphic unit contains of depositional system that together reflect the paleogeography through an interval of basin history. Each depositional system consists of facies associations which commonly show repetitive development in successions of stacked cycle. In this thesis report, the sequence stratigraphic interpretation is limited within main reservoir interval in Pari field. The sequence stratigraphic interpretation is based on the well data and 3D seismic data. A geostatistical method used in this thesis work to model the 3D facies distribution through the study area but limited only for the main reservoir unit in the Pari field. The goal is to capture all of the correctly scaled reservoir characteristics based on the available well data and 3D seismic data.

## **1.3 Thesis Structure**

The overall thesis is comprised of five chapters. Chapter 1, Introduction is states the thesis objectives and describes available datasets used in this thesis work. In Chapter 2, provides the description of geological setting and sequence stratigraphy concept in submarine fan systems. Chapter 3, provides the description of geostatistical method to integrated well and seismic data. In Chapter 4, describes the application to real datasets in Pari field, offshore East Kalimantan, Indonesia. Finally, the conclusion for the present work and recommendations for future work are provided in Chapter 5.

## 1.4 Available Datasets

Available data sets used for this thesis research are:

1. 3D seismic volume (Post-Stack Depth Migration/PSDM) covers area about 313 km<sup>2</sup> and consists of 1,683 inlines and 1,189 crossline. Seismic line interval has 12.5 meters spacing.
2. Wireline log data from Pari-1, Pari-2, Pari-3 and Pari-5 wells. Wireline log data was gathered through LWD (Logging While Drilling). The type of log data gathered is included: gamma ray, resistivity, density, neutron, and sonic. In general, the log data has excellent quality because of minimum magnitudes of washout, tool pulls and filtrate invasion.
3. Sedimentology and special core analysis report of conventional core data from Pari-2 and Pari-5 wells. Core data in Pari-2 well has total length approximately 320 feet and Pari-5 well has total length approximately 182 feet.

## 1.5 Software and Hardware used

*Petrel Schlumberger* software was used as main geological and geophysical software for well log analysis, well log correlation, seismic interpretation, data analysis and 3D reservoir modeling. *Veritas Hampson-Russell* software (Emerge module) was used to performed seismic multiattribute analysis. *Microsoft Word* and *Microsoft Power Point* was used for thesis report and presentation slide. The hardware used for this thesis project has minimum configuration for processor 1 GHz, internal memory 1 Gb, and graphic card 128 Mb.



## Chapter 2

# Geological Setting and Sequence Stratigraphy Concept

### 2.1 Pari Field Geography

The Pari Field is located in the Makassar Strait, offshore East Kalimantan, Indonesia within the Ganai Production Sharing Contract (PSC) operated by Chevron Indonesia Company. The field lies between 3,500 – 5,500 feet of water depth on the continental slope of the southern Mahakam Delta approximately 80 kilometers to the Southeast direction (Figure 2.1).



Figure 2.1 Pari Field is located in the Makassar Strait, southern Mahakam Delta, offshore East Kalimantan (picture taken from goggle earth website).

## 2.2 Pari Field Geological Setting

The Pari Field is located in the Makassar Strait which lies between the island of Borneo and Sulawesi. Makassar Strait was rifted apart during the Early Eocene and the strait is divided into several basins, the Kutai Basin which extends onshore into Borneo, the North Makassar Basin and the South Makassar Basin. The study area is located in the Kutai Basin which has been receiving clastics sediment from the Borneo to the east, primarily from the Mahakam River. The Kutai Basin covers an extensive area of about 60,000 km<sup>2</sup>. The Kutai Basin is bounded to the south by the Paternoster Platform, a primarily carbonate platform with relatively shallow water conditions since the Eocene. The Paternoster is separated from the Kutai Basin by the Adang fault system which was likely a transform during initial rifting and since reactivated in oblique slip due to later compression and relative subsidence of the Kutai Basin. To the north the basin is bounded by the Mangkalihat Peninsula, and elevated block extending offshore to Sulawesi. The Mangkalihat block has experienced shallow to deepwater conditions during the early Miocene with a variable and complex uplift history. To the west, the basin limit is confined by the Kalimantan central range or Kuching uplift and to the east the Kutai Basin passes into the deep-marine Makassar Strait (Figure 2.2).

The tectonic stage in the Kutai Basin is divided into three main stages: Stage I. Syn-rift (middle-late Eocene), Stage II. Sagging (late Eocene-early Miocene) and stage III. Deltaic (early Miocene-recent). The syn-rift stage was initiated in the middle Eocene with an extensional rift phase associated with sea-floor spreading in the Makassar Straits. The half-grabens that developed at this time filled with middle to late Eocene syn-rift sediments. Stage II of sagging initiated during the late Eocene while the basin deepening produced marine conditions throughout. The marine deposits include carbonates and deep marine turbidities. The carbonates were more widely developed on the basin flanks and basement highs. The

center of the basin filled with turbidites and deep marine shales. The last Deltaic stage initiated during early Miocene. The early Miocene deepwater conditions persisted in the basin center and carbonates continued to develop on the basin flanks prior to the onset of late-early Miocene inversion, when uplifted Eocene and Oligocene sediments were eroded and a major delta system formed in the west and prograded to the east. Deltaic sedimentation continued into the middle and late Miocene, punctuated by compressional deformation, uplift and erosion in response to basin inversion. The middle-late Miocene also represents the period when delta-plain to delta-front coals and carbonaceous shale source rock for the Mahakam and deepwater hydrocarbon were deposited.

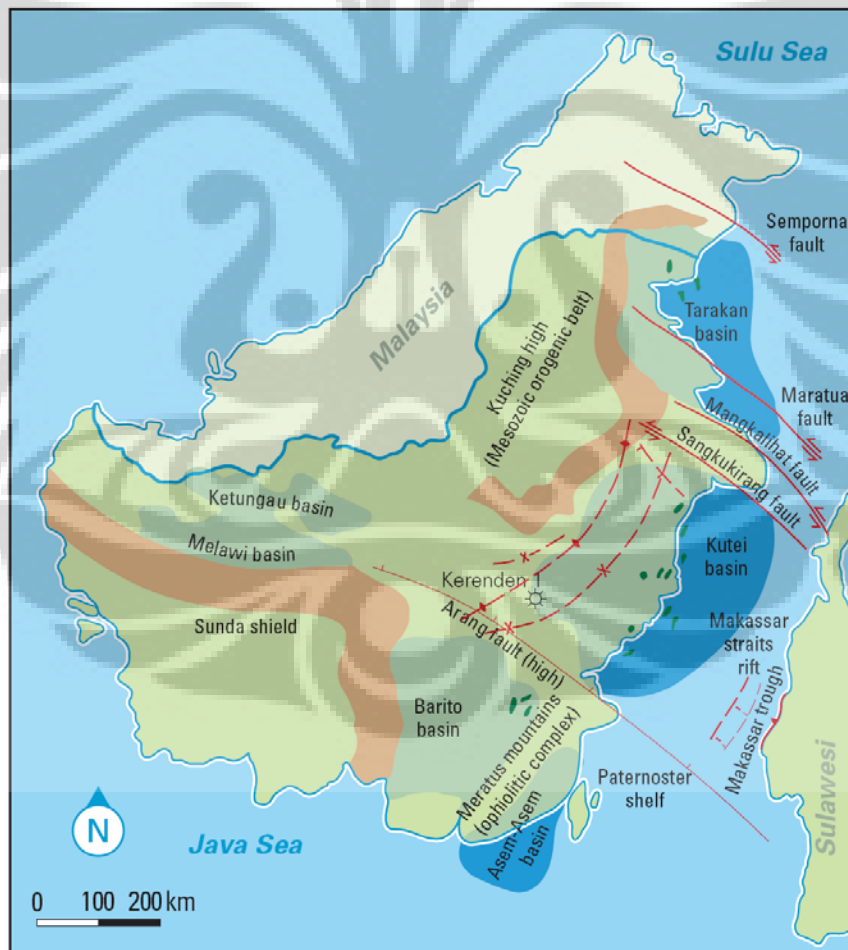


Figure 2.2 Geological setting of Kutai Basin with distribution of hydrocarbon fields (adapted from Mamuya et al., 1995).

Compressional folding continued throughout the Pliocene and Pleistocene and formed the long, sinuous, sub parallel anticlines that have trapped hydrocarbons in the predominantly deltaic Miocene reservoirs. The latest successes has been in the deepwater slope Mahakam Delta area where the Miocene, lowstand, turbidite submarine fans deposits host significant oil and gas discoveries including in the study area.

### **2.3 Pari Field Stratigraphy**

Stratigraphic age of the main reservoir in Pari Field is middle to late Miocene. The total depth (T.D) of the wells used in this study is in the Miocene section. Below well penetration, regional correlation indicates a continuous section through areally extensive Oligocene shale to an Eocene syn-tectonic section associated with initial basin opening. The uppermost couple hundred feet of section comprises a Pleistocene to Recent drape deposit. The Pleistocene section is marked by widespread sandy intervals associated with sea-level low stands. Below the Pleistocene section is regional shale underlain by a sequence of interbedded Pliocene sand and shale. The Pliocene section above the main Pari field is water wet, however; this interval contains gas pay in nearby wells. Below the Pliocene sands is a thick shale section that serves as a top seal for the main reservoir in the field (Figure 2.3).

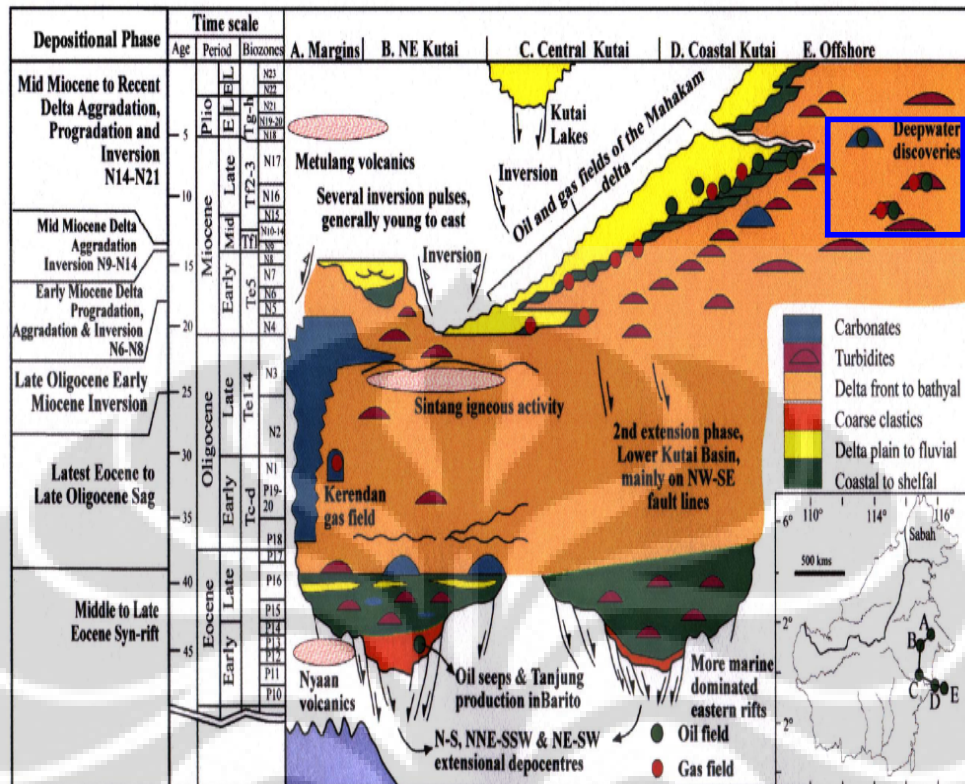


Figure 2.3 Tectonostratigraphy of Kutai Basin, blue box showing relative stratigraphic position of the objective reservoir (adapted from Moss et al., 1999).

## 2.4 Seismic Sequence Stratigraphy Concept

Seismic stratigraphy is basically a geologic approach to the stratigraphic interpretation of seismic data. The unique properties of seismic reflections allow the direct application of geologic concepts based on physical stratigraphy. Primary seismic reflections are generated by physical surfaces in the rocks, consisting mainly of stratal (bedding) surfaces and unconformities with velocity-density contrasts. Therefore, primary seismic reflections parallel stratal surfaces and unconformities. Whereas, all the rocks above a stratal or uniformities surfaces are younger than those below it, the resulting seismic section is a record of the chronostratigraphic (time-stratigraphic) depositional and structural patterns and not a record of

the time-transgressive lithostratigraphy (rock-stratigraphy). Seismic reflection terminations and configurations are interpreted as stratification patterns, and are used for recognition and correlation of depositional sequences, interpretation of depositional environment, and estimation of lithofacies. Seismic sequence analysis subdivides the seismic section into packages of concordant reflections, which are separated by surfaces of discontinuity defined by systematic reflection terminations. These packages of concordant reflections (seismic sequences) are interpreted as depositional sequences consisting of genetically related strata and bounded at their top and based by unconformities or their correlative conformities. Reflection terminations interpreted as stratal terminations include erosional truncation, toplap, onlap, and downlap.

Top-discordant relations include erosional truncation and toplap. Erosional truncation implies the deposition of strata and their subsequent removal along an unconformity surface. Interpretation of reflection terminations as erosional truncation maybe straight forward or quite subjective, depending on the angularity of the reflections to the erosional surface. In some instances, the erosional surfaces itself may produce a seismic reflection; elsewhere there is no reflection from the surface only the systematic terminations of underlying reflections may define the surface. In general, however, erosional truncation is the most reliable top-discordant criterion of the sequence boundary. Toplap is the termination of reflections interpreted as strata against an overlying surface as a result of non deposition (sedimentary by passing) and only minor erosion. In practice, many depositional boundaries marked by toplap are found to be rather local extent, and in many cases can not be correlated regionally. For this reason, minor occurrences of toplap are commonly included within mapped depositional sequences and at their upper boundaries.

Base-discordant relations include seismic onlap and downlap. Onlap is a relation in which seismic reflections are interpreted as initially horizontal

strata terminating progressively against and initially inclined surface, or as initially inclined strata terminating progressively updip against a surface of greater inclination. Downlap is a relation in which seismic reflections are interpreted as initially inclined strata terminating downdip against an initially inclined or horizontal surface. If onlap can not be distinguished from downlap because of subsequent deformation, the more inclusive term baselap maybe necessary.

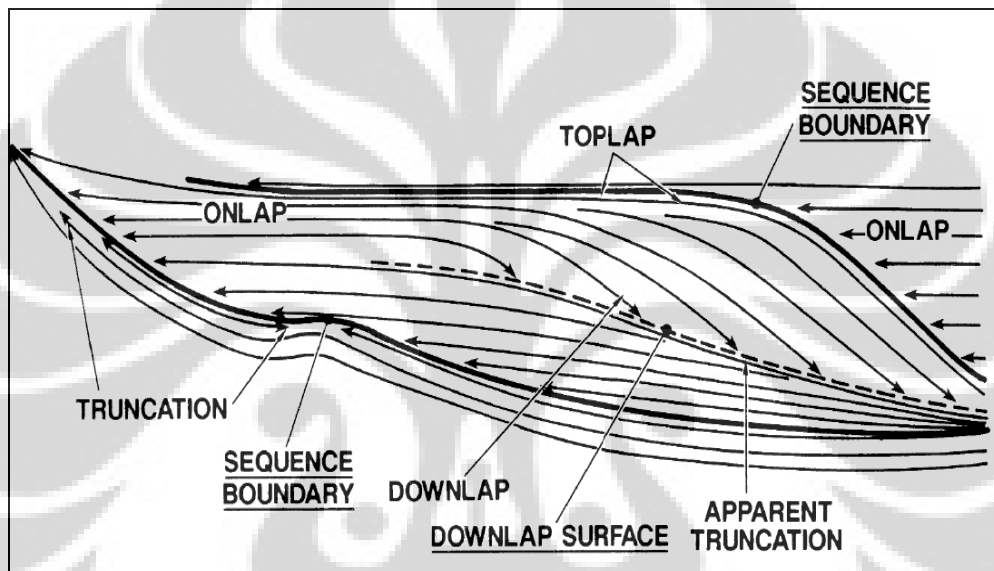


Figure 2.4 Diagram showing reflection termination patterns and type of discontinuities (adapted from Mitchum and Vail, 1977).

After seismic sequences are defined, environment and lithofacies within the sequence are interpreted from seismic and geologic data. Seismic facies analysis is the description and geologic interpretation of seismic reflection parameter, including configuration, continuity, amplitude, frequency, and interval velocity. Description and interpretation of reflection configurations begin with simple patterns and continue to the more complex. Variations within configurations commonly can be described with modifying terms such as: Parallel and sub parallel, divergent, prograding reflection configuration, sigmoid progradational configuration, oblique progradational reflection configuration, complex sigmoid-oblique progradational reflection configuration, shingled, and hummocky clinoform.

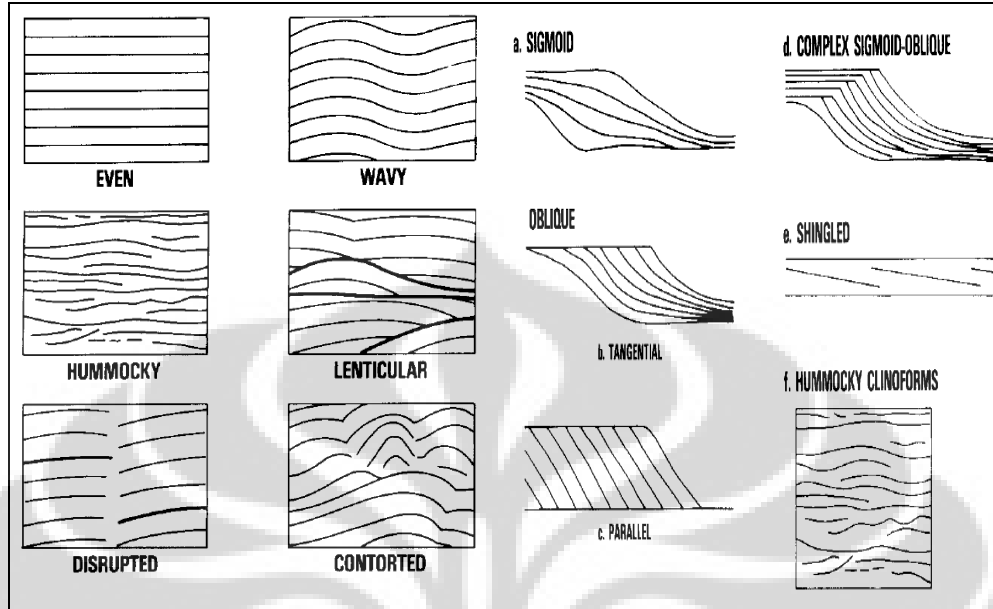


Figure 2.5 Type of seismic reflection pattern and configuration within sequences (adapted from Mitchum and Vail, 1977).

## 2.5 Models for Submarine Fan Deposition within a Sequence Stratigraphic Framework

Submarine fans are defined as “terrigenous, cone-or fan-shaped deposits located seaward of large rivers and submarine canyon”. This physiographic feature can form at any time if conditions are right. These conditions include:

1. Presence of slope length sufficient to allow significant gravity flows and turbidity currents to develop.
2. Abrupt delivery of relatively coarser grained sediment to the outer shelf an upper slope resulting in inherently unstable conditions.
3. Instability of the outer shelf and upper slope caused by seismic events or gradual depositional build-up.
4. Interception of longshore drift by submarine canyons.



Fans are composed typically of turbidite deposits delivered to deepwater by sediment gravity flows. Posamentier and Vail (1985, 1988) discuss the stratigraphic response to eustatic change and describe in detail the conceptual framework on which sequence stratigraphy is based. The rate of subsidence was assumed to be uniform over a single cycle of eustatic change and that during this time a sequence bounded by unconformities and composed of a predictable succession of depositional systems tract is formed. The exact timing of the deposition of each systems tract is largely a function of local tectonics as well as sediment supply integrated with eustatic change. Using the Posamentier and Vail's (1985, 1988) sequence stratigraphic terminology, sediments deposited during intervals of relative sea-level fall and subsequent lowstand are referred to as the lowstand system tract. This system tract is subdivided into two component parts that are not coeval: lowstand fan and the lowstand wedge. The lowstand fan is deposited during interval characterized by falling relative sea level, whereas the lowstand wedge is deposited during subsequent slow relative submarine fans deposition whose depocenter occurs on the basin floor. Within the lowstand wedge, the depocenter for submarine-fan deposits shifts to the slope. The three component parts of the lowstand systems tract are: the lowstand fan, the early lowstand wedge or channel-levee complex, and the late lowstand wedge or prograding complex.

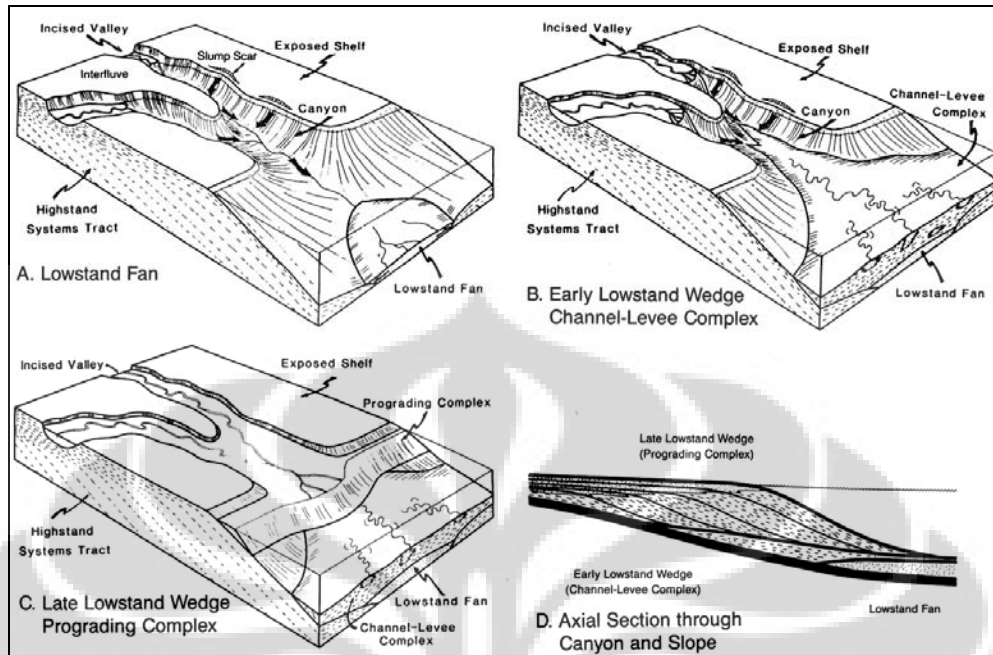


Figure 2.6 Conceptual block diagrams of the lowstand system tract: (A) lowstand fan, (B) early lowstand wedge (channel-levee complex), (C) late lowstand wedge (prograding complex), and (D) an axial section through the canyon and slope (adapted from Posamentier and Vail, 1985, 1988).

### 2.5.1 Lowstand Fan

Initiation of lowstand fan deposition occurs when two requisite criteria are fulfilled: (1) rate of eustatic fall exceeds rate of total subsidence or rate of tectonic uplift exceeds rate of eustatic rise at the physiographic shelf/slope break resulting in a relative sea-level fall, and (2) progradational shelf deposition has reached the shelf/slope break during the preceding sea-level highstand or the depocenter has shifted to the shelf edge by sea level fall. The interaction between eustacy and subsidence to produce relative sea-level variations is illustrated in Figure 2.7. At position “A” on the relative sea level curve, the rate of eustatic fall equals the rate of total subsidence and the rate of relative sea-level change is zero. Prior to this time deposition of the highstand systems tract occurs. During the interval between “A” and “B”, relative sea level falls and in response fluvial systems and canyons incise and the lowstand fan unit of the lowstand

systems tract is deposited. At position “B” on the relative sea-level curve, the rate of eustatic fall again equal the rate of total subsidence, hence the rate of relative sea-level change again to zero. Subsequently, relative sea level slowly rises resulting in deposition of the early and late lowstand-wedge unit of the lowstand systems tract.

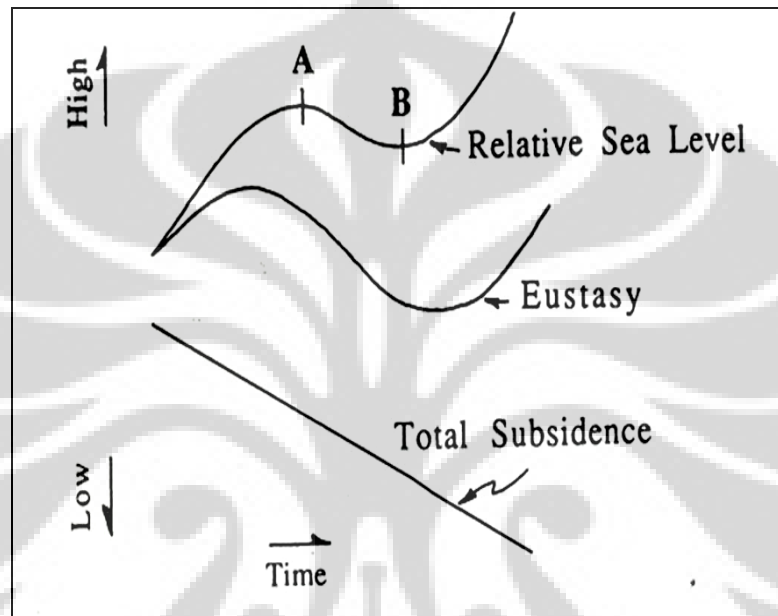


Figure 2.7 Relative sea levels as a function of eustasy and total subsidence (thermal cooling, tectonics, sediment loading and compaction).

During the interval of relative sea-level fall, canyons and incised valleys are cut progressively deeper as base level continues to fall. Within the canyons, sediment gravity flows tend to keep the system flushed of any sediment that may be supplied by stream bed load delivery, failure of the canyon head or canyon walls, or other mass movement processes. The canyons, which are actively deepening and serving as sediment conduits, are zone of bypass at this time. Sediments transported through the canyons are ultimately deposited as turbidites where abrupt decreased in slope gradient occur, whether this is on the basin floor or on the slope within intraslope basins.

## 2.5.2 Lowstand Wedge

Lowstand wedge deposition is initiated as lowstand fan deposition ends. This occurs when relative sea level rise at the shelf edge begins. At this time relative sea level is at its lowest position and subsequently begins to rise slowly. Although eustatic fall may continue at this time, the rate of fall is decreased to less than the rate of subsidence. In response, stream incision ceases as base level slowly rises. The grain size distribution of the sediment delivered to the upper slope changes as well, as the coarser grain fraction is preferentially deposited within the incised valley. Consequently, the sand to mud ratio of the sediment delivered to the upper slope decreases greatly. The lowstand wedge is characterized by deposition within incised valleys as well as on the slope and in the basin. Within lowstand wedge, two subunits can be sometimes identified: the early lowstand wedge or channel-levee complex and the late lowstand wedge or prograding complex. Both are coeval with incised valley fill on the shelf and both may be fan shaped in the lower parts of the slope and basin. The difference between deposition during lowstand fan and lowstand wedge time are summarized in Figure 2.8 below. Low stand fan time occurs during relative sea level falls while lowstand wedge, which composed of two sub-unit, the early lowstand wedge (channel-levee complex) and the late lowstand wedge (prograding complex), is initiated when relative sea level stops falling and begins to rise slowly.

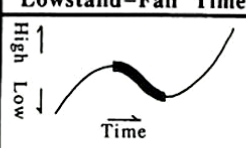
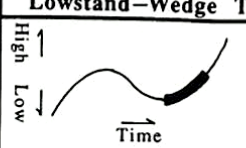
	Lowstand-Fan Time	Lowstand-Wedge Time
Relative Sea Level		
Stream Base Level	Falling	Rising
Fluvial Regime	Incising/Eroding	Filling/Depositing
Sand:mud Ratio Delivered to Upper Slope	High	Moderate
Canyons	Cutting	Filling
Principal Depocenter	Basin, Lower Slope	Incised Valleys, Outer Shelf, Upper Slope
Principal Turbidite System (after Mutti, 1985)	Type I, II	Type II, III

Figure 2.8 Characteristics of lowstand fan and lowstand wedge time (adapted from Posamentier and Vail, 1985, 1988).

## 2.6 Element of Submarine Fan Systems

Elements are defined as the basic mappable component of both modern and ancient turbidite systems. Elements can have depositional and/or erosional characters. Depositional elements are characterized by a distinctive assemblage of similar facies and facies associations that permit differentiation from adjacent strata that bound them both vertically and laterally. Erosional elements are particularly well expressed in modern fans and can also have a distinctive seismic expression in the subsurface. The five major elements are: (1) Major erosional features (excluding channels), (2) Channels, (3) Overbank deposits, (4) Depositional lobes, and (5) Channel-lobe transition deposits and related morphologic features.

### (1) Major erosional features

This element includes number of large-scale erosional features that are particularly well expressed in modern fan systems as well as in the seismic

expression of some ancient systems. These features include (1) shelf-edges failures, (2) slope failures, (3) failures within the basin turbidites, and (4) canyon. The fill of these large-scale erosional features is highly variable and generally quite complex because they are commonly related to repeated periods of erosion and sedimentation (Mutti, 1985). In the modern systems, these features still contain significant remnants of the original slide events and in the ancient systems, the fill is generally composed of either predominantly prograding delta-slope or deltaic deposits. The fill of these erosional features is therefore largely represented by strata that are part of stages of growth of the turbidite systems that are younger than the stages that produced the erosional feature.

## (2) Channels

Channels are elongate negative relief features produced and/or maintained by turbidity-current flows. Channel shape and position within a turbidite system are controlled either by depositional processes in the case of those associated with large levee/overbank wedges or by erosional down cutting, especially where the channel relief can be dominantly erosional or depositional in origin or can result from a combination of both processes. There are two main types of channels on modern submarine fans: large, leveed valleys that are the primary sediment feeder systems (generally connected to a canyon upstream) and smaller, commonly unleveed channels that appear to function as distributaries. There are three channel types in ancient channel-fill deposits which include sedimentary packages that formed within the channels after these erosional features ceased to act as effective sediment transport pathways (Figure 2.9). Those types are: (1) Erosional channel-fill deposited with basal, coarse grained residual facies overlain by fine grained, channel abandonment deposits. (2) Depositional channel-fill deposits are primarily made up of depositional facies that infilled the channel after its main phase of activity as a pathway for sediment transport. (3) Mixed channel-fill

deposits are transitional between these two types or result from a switch between types. Ancient channel-fill sequences generally occur as composite features resulting from the vertical stacking and lateral juxtaposition of several channel-fill units. These composite features rarely exceed a thickness of a hundred meters and widths of a few kilometers and have a very complex internal structure probably recording both allocyclic and autocyclic mechanism of deposition.

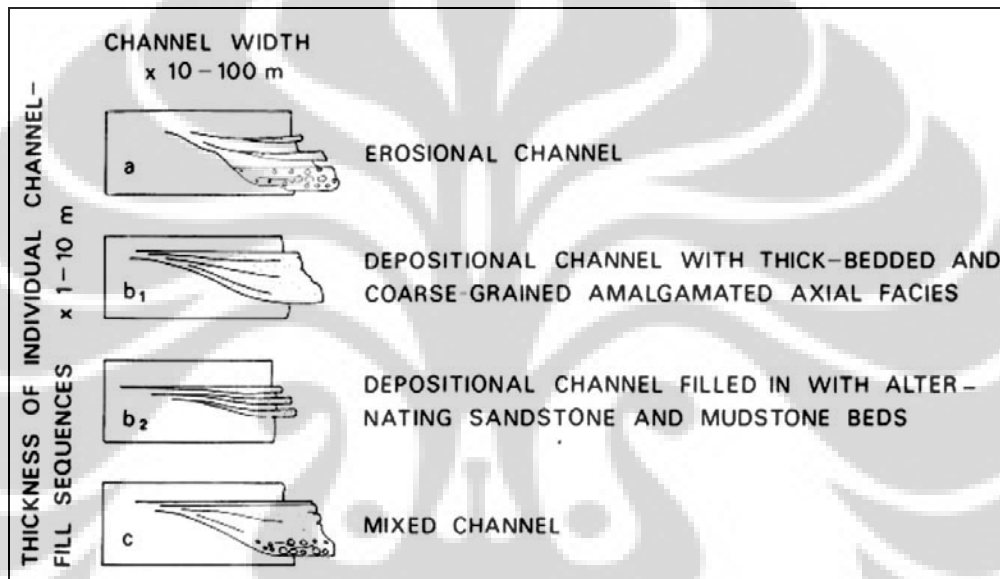


Figure 2.9 Main types of channel-fill deposits observed in ancient turbidites. Vertical scale ranges from several meters to tens of meters and horizontal scale ranges from tens of meters to hundreds of meters (adapted from Mutti and Normark, 1987).

### (3) Overbank deposits

Overbank deposits are generally fine-grained, thin-bedded turbidite sediments that can be laterally extensive and are adjacent to the main channels in a turbidite system. The areas of Overbank deposition on most modern systems can be subdivided into two parts: (1) those with levee relief, where Overbank deposition along the margins of an active channel has constructed positive relief and (2) the more distal parts of the Overbank environment without major relief. Ancient Overbank deposits are fairly easy to recognize in both outcrop and seismic data. Ancient

Overbank deposits can be subdivided into two main groups: (1) channel-related Overbank deposits and (2) Overbank wedges (Mutti and Normark, 1987). The first group includes a variety of thin-bedded and fine-grained turbidite sandstone facies that occur within channels/thalweg, along the edges of channels, and within interchannel areas. The second group is characterized by a thick wedge of fine-grained, mainly muddy turbidite beds that are as much as several hundred meters thick near the margins of the basin and gradually wedge-out in a basinward direction over distances of tens of kilometers into thin mudstone units that are probably of basin wide extent.

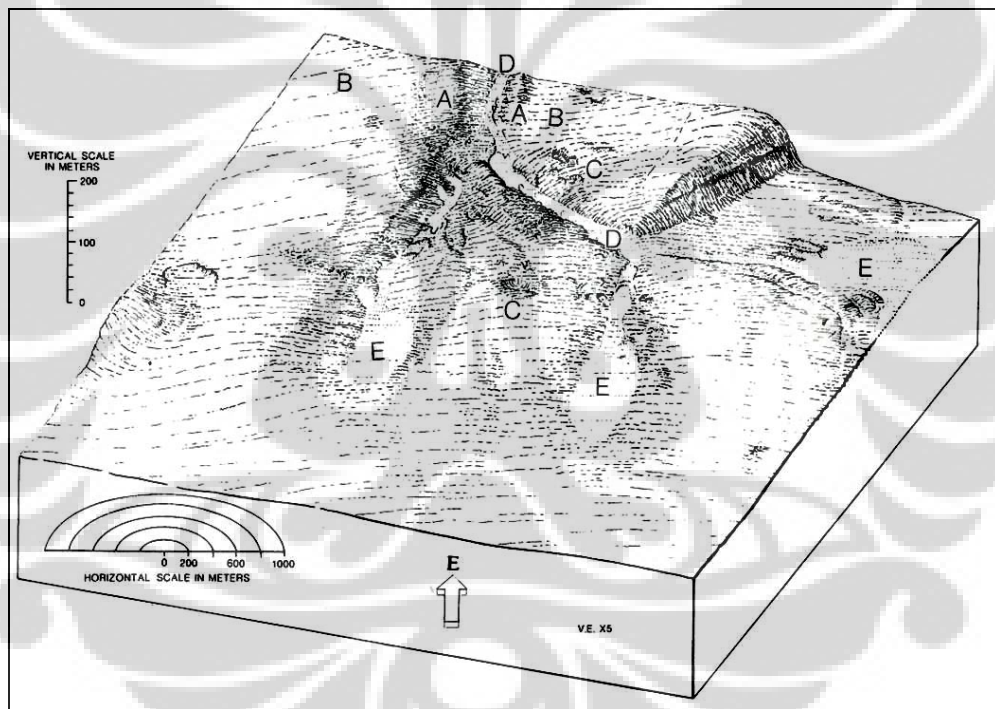


Figure 2.10 Physiographic map of submarine fan showing (A) levee, (B) distal overbank, (C) large scale scours, (D) channel floor, and (E) depositional lobes (adapted from Normark et al., 1980).

#### (4) Depositional lobes

Depositional lobes are represented by roughly tabular, nonchannelized bodies that have individual thicknesses generally of 3-15 m. Each lobe is made up of relatively thick and coarse sandstone beds. Individual



sandstone lobes in ancient systems commonly form vertical successions as much as several hundred meters thick, in which the sandstone bodies alternate with variable thicknesses of mudstone and thinner bedded and finer grained sandstone. The sand/mud ratio observed in these successions may vary considerably from one system to another and also in different stratigraphic interval within the same system. The extent of the lobe generally varies from a few kilometers to several tens of kilometers. Sandstone lobes can thus be basin-wide features with abrupt onlap terminations against the basin margin as well as roughly tabular bodies that gradually thin and shale-out into peripheral thinner bedded lobe-fringe deposits. In any given system, the sandstone lobes represent the maximum down current extent of the sand transported to the basin. Sandstone lobes also contain scours, but they are neither as deep nor as abundant as those observed in the channel-lobe transition deposit or in some channel-fill sequences. The scours tend to be flat-floored and have sharp, step-like edges. As the result of scouring processes, sandstone lobes contain abundant amalgamation surfaces and outsize rip-up clasts, particularly in the more proximal sectors.

#### (5) Channel-lobe transition deposits and related morphological features

This element is of fundamental importance to understand the depositional setting and facies distribution of turbidite systems and their component stages. The main features that characterized ancient channel-lobe transition deposits include: (1) extensively scoured and amalgamated sandstone and pebbly sandstone facies, (2) coarse-grained and lenticular, cross stratified sandstone beds, (3) abundant outsize rip-up mudstone clasts, and (4) a variety of scours and cut and fill-deposits.



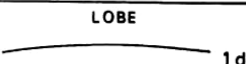
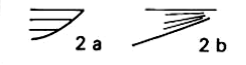

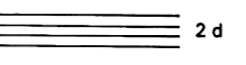
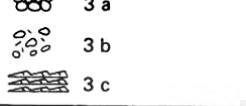


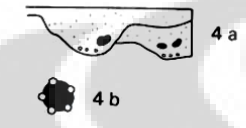
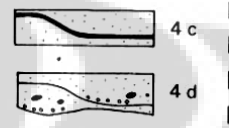
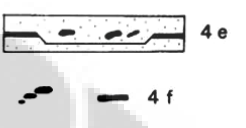
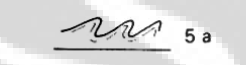
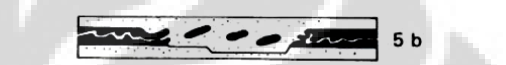
	CHANNELS	TRANSITION	LOBES
<b>MORPHOLOGIC EXPRESSION</b>	 CHANNELS	 ROUGHNESS	 LOBE
<b>BEDDING PATTERN (Outcrop scale)</b>	 2 a 2 b	 2 c	 2 d
<b>DEPOSITIONAL FEATURES</b>	 3 a 3 b 3 c	 3 d 3 e	 3 f
<b>EROSIONAL FEATURES and OUT-SIZE MUDSTONE CLAST</b>	 4 a 4 b	 4 c 4 d	 4 e 4 f
<b>CHAOTIC UNIT</b>	 5 a	 5 b	
<b>OTHER FEATURES</b>	SHALLOW WATER TRACE FOSSILS LOCALLY COMMON		COMPENSATION CYCLES

Figure 2.11 Main characteristic features of channel, channel-lobe transition, and lobe deposits (adapted from Mutti and Normark, 1987).

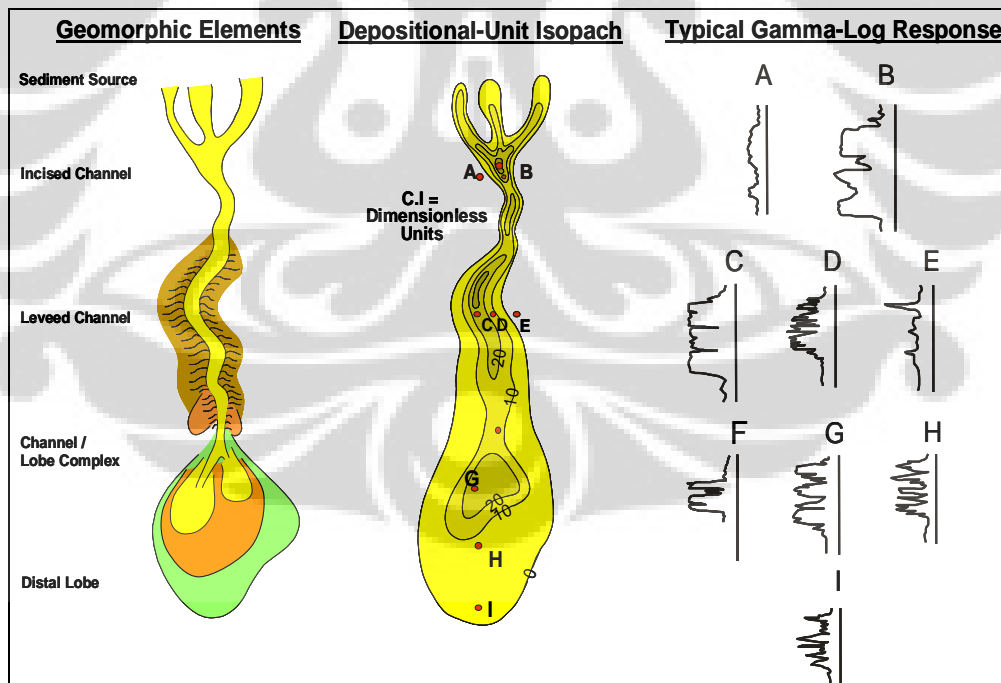


Figure 2.12 Geomorphic elements, depositional unit Isopach, and log responses of a channel-lobe complex (adapted from Galloway, W.E., and D.K. Hobday, 1996).

## Chapter 3

# Geostatistical Integration of Well and Seismic Data

### 3.1 Introduction

Predicting rock and reservoir properties is an essential task in hydrocarbon exploration and development. It is crucial in estimating oil and gas reserves and planning future production operations. Geophysical and geological measurements in hydrocarbon exploration and development can be divided into two major categories: measurement at the well locations (well logs and core samples information) and seismic data. The integration of these data is not an easy task since they have different characteristics. Geological and reservoir models are usually created based on sparse well data heavily depend on the well locations. This can lead to poor estimation, especially in geologically complex areas. On the other hand, 3D seismic data can provide good coverage spatially over the exploration area, but have limitations associated with noise levels, band-limited frequency spectra, phase errors, and significantly lower vertical resolution compared to well data.

Conventional methods for estimating rock and reservoir properties from well logs and seismic data rely on empirical or regression formulas. Such approaches treat the data as spatially independent observations and ignore the existence of spatial patterns. Geostatistical methods have the important ability to integrate different types of information into a consistent subsurface model. They provide improved reservoir description, considering the spatial correlation of geophysical data and add the ability to assess the uncertainty in the estimation process.

## 3.2 Reservoir Facies Modeling

### 3.2.1 Seismic Multiattribute Method

The idea of using multiple seismic attributes to predict log properties was first proposed by Schultz, Ronen, Hattori and Corbett in a series of three articles in the Leading Edge. (Seismic-guided estimation of log properties, Parts 1, 2 and 3 by Schultz et al, The Leading Edge, May, June and July, 1994). In these articles, they point out that the traditional approach to using seismic data to derive reservoir parameters has consisted in looking for a physical relationship between the parameter to be mapped and some attribute of the seismic data, and then using that single attribute over a 2D line or 3D volume to predict the reservoir parameter. Although relationships have been inferred between these attributes and reservoir parameters, the physical basis is not always clear, and they proposed deriving statistical, rather than deterministic, relationships.

Given a particular attribute of the seismic data, the simplest procedure for deriving the desired relationship between target data and seismic attribute is to crossplot the two. Figure 3.1 shows an example in which a target log property, in this case density-porosity, is plotted against a seismic attribute. The assumption is that the target log has been integrated to travel time at the same sample rate as the seismic attribute. Effectively, this integration reduces the target log to the same resolution as the attribute, which is usually significantly coarser than the log property. Each point in the crossplot consists of a pair of numbers corresponding to a particular time sample. Assuming a linear relationship between the target log and the attribute, a straight line may be fit by regression:

$$y = a + bx. \tag{3.1}$$

The coefficients  $a$  and  $b$  in this equation may be derived by minimizing the mean-squared prediction error:

The extension of the conventional linear analysis to multiple attributes (multivariate linear regression) is straightforward. Assume, for simplicity, that we have three attributes as shown in Figure 3.2. At each time sample, the target log is modeled by the linear equation:

$$L(t) = w_0 + w_1A_1(t) + w_2A_2(t) + w_3A_3(t). \quad (3.2)$$

As shown in the Appendix, the solution for the four weights produces the standard normal equations: Just as in the single-attribute case, the mean-squared error (10) calculated using the derived weights constitutes a goodness-of-fit measure for the transform, as does the normalized correlation, where the x-coordinate is now the predicted log value and the y-coordinate is the real log value.

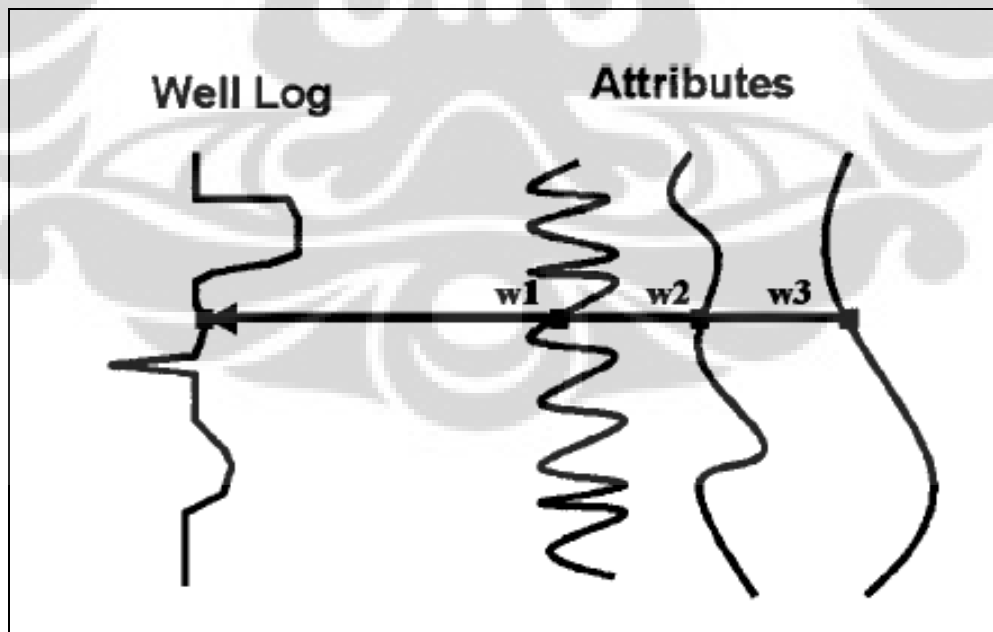


Figure 3.1 Assuming the case of three seismic attributes, each target log sample is modeled as a linear combination of attribute samples at the same time.

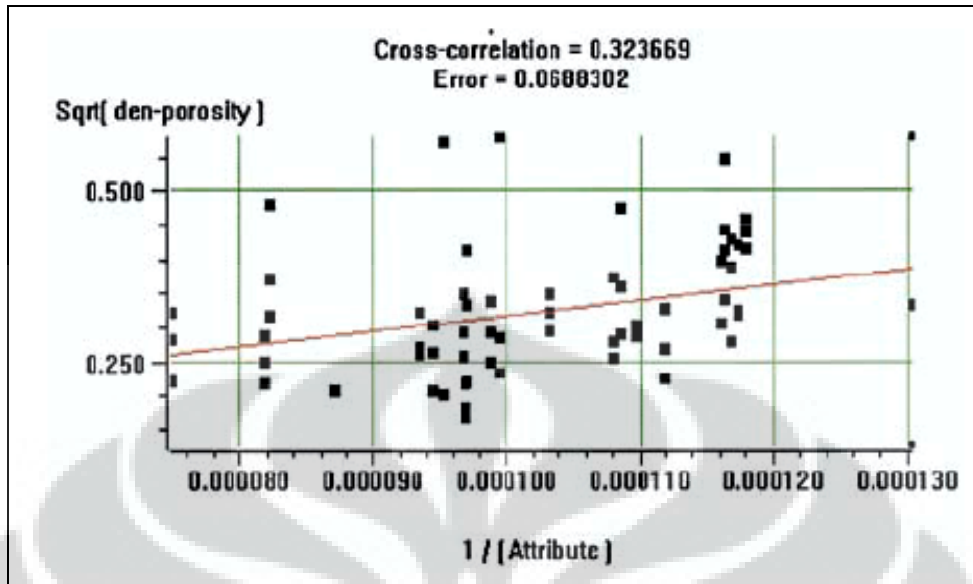


Figure 3.2 Applying nonlinear transforms to both the target and the attribute data improves the correlation between the two.

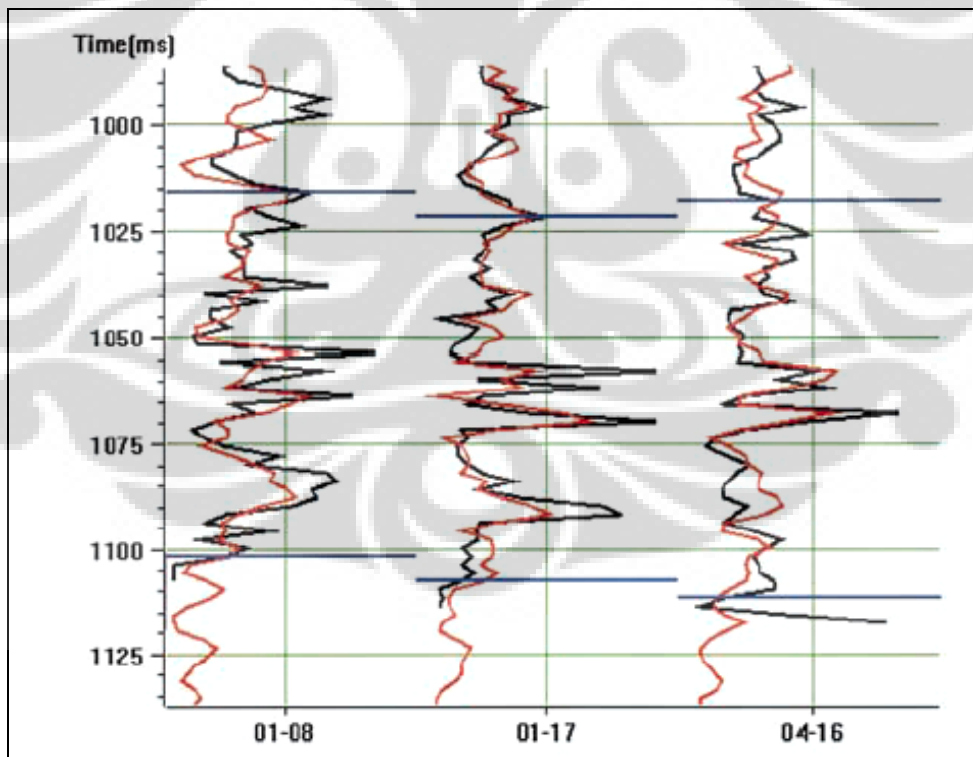


Figure 3.3 Applying the multiattribute transform using six attributes and a seven-point operator. Only the first three wells are shown. The original porosity log is shown in black; the predicted log is shown in red. The normalized correlation coefficient for all the wells is 0.69.

### **3.2.2 Object Based Modeling Method**

Object based modeling method is one of the techniques available for generating 3D stochastic models. The Norwegians pioneered the development of object based models, which produced satisfactory representations of the distribution of channels in fluvio-deltaic formations within some of their giant fields. Object based modeling assume that the various facies are associated with well defined geometries and their size (width, length, thickness) is random and can be statistically quantified by the geologist. Object based simulations can also incorporate constraints about the relative position of different geological objects. For instance, crevasse splays which result from sediment spills on the edges of channel, must always be located close to a channel. Trend can also be incorporated for controlling the proportion of various objects vertically or spatially. Object based simulation algorithms work easily in situations where the well spacing is much greater than the lateral dimension of the modeled objects. However, conditioning is much more difficult when sand body dimensions are large compared with well spacing because well to well geological correlations are difficult to handle.

### **3.2.3 Variogram – a measure of spatial variability**

The variogram is the key function in geostatistics as it will be used to fit a model of the spatial/temporal correlation of the observed phenomenon. If we view some measured data points on a map, we can often see that low values tend to be near other low values and high values tend to be near other high values, i.e. there is an existing spatial continuity in the dataset. Two data points close to each other are more likely to have similar values than two points that are far apart. The dissimilarity between all the data pairs can be expressed by the variogram as a function of the distance  $h$ , often called offset or lag, between them. The variogram for lag distance  $h$

is defined as the average squared difference of values separated approximately by  $h$ , and can be written as

$$\gamma(h) = \frac{1}{N(h)} \sum_{i=1}^{N(h)} [Z(x_i) - Z(x_i + h)]^2 \quad (2.1)$$

Where  $N(h)$  is the number of all pairs separated by distance  $h$ .

If two different properties have been measured,  $Z$  and  $Y$ , the measure of variability is the cross-variogram, defined by

$$\gamma(h) = \frac{1}{N(h)} \sum_{i=1}^{N(h)} [Z(x_i) - Z(x_i + h)][Y(x_i) - Y(x_i + h)] \quad (2.2)$$

The computation of the cross-variogram requires collocated measurements of the two properties.

In practice, we usually separate the data points into a number of offset bins and compute the variogram value in each bin. In this case,  $h$  defines the offset to the center of the bin. The direct use of the variogram in geostatistical techniques can lead to some mathematical complications, for example singular matrices, multiple solutions, or negative mean-square errors (Isaaks and Srivastava, 1989). The variogram values are computed for all pairs of sample locations, but the geostatistical techniques require a variogram value between all the sampled locations and the locations we wish to estimate. Therefore, we require a variogram model which is a function of the offset  $h$ . The model cannot be an arbitrary function, it must obey certain rules (Isaaks and Srivastava, 1989). The model is defined by second-order stationarity: the expected value is constant over the area and the variogram depends on the length and the orientation of offset  $h$ , but not on its position  $x$ . Figure 3.4 is a typical example of a computed (experimental) variogram and a model (theoretical) variogram fit to it. The offset distance at which the model flattens off to a plateau is called range. This value defines the distance at which the differences between the wells become random, i.e. they are not spatially related. The value of the



plateau is called the sill. Note that a non-zero value, called nugget, can be added to the model at zero offset.

The most commonly used variogram models in practice are:

- Spherical, defined by:

$$\begin{cases} \gamma(h) = C[1.5(h/a) - 0.5(h/a)^3] & h \leq a \\ \gamma(h) = C, & h > a \end{cases} \quad (2.3)$$

- Exponential, defined by:

$$\gamma(h) = C[1 - \exp(-h/a)] \quad (2.4)$$

- Gaussian, defined by:

$$\gamma(h) = C[1 - \exp(-h/a)^2] \quad (2.5)$$

- Power, defined by:

$$\gamma(h) = Ch^n \quad (2.6)$$

where  $a$  is the range and  $C$  is the sill.

The covariance function can be computed from the variogram

$$\sigma(h) = \gamma(\infty) - \gamma(h) = \sigma(0) - \gamma(h) \quad (2.7)$$

where  $\gamma(\infty)$  is the sill value and  $\sigma(0)$  is the zero-offset covariance.

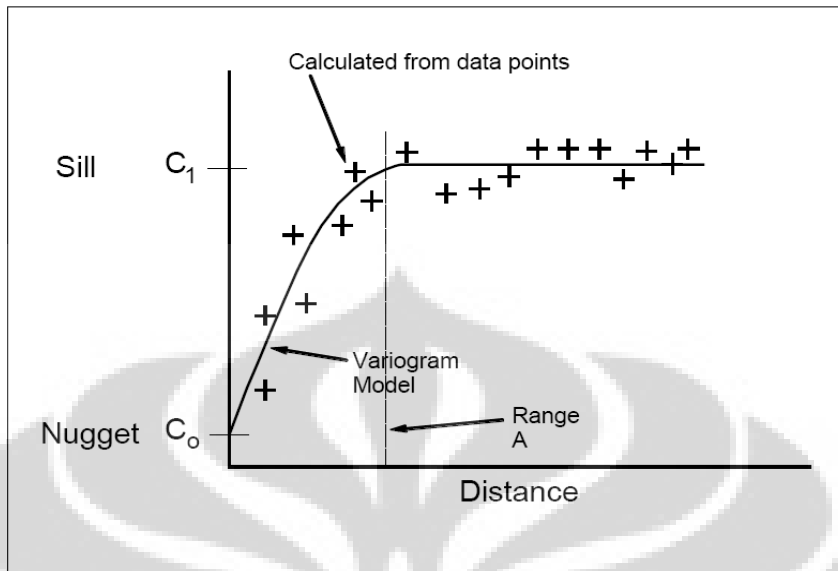


Figure 3.4 Parts of a variogram. The nugget quantifies measurement inconsistency and the range is the break point between correlated and uncorrelated data.

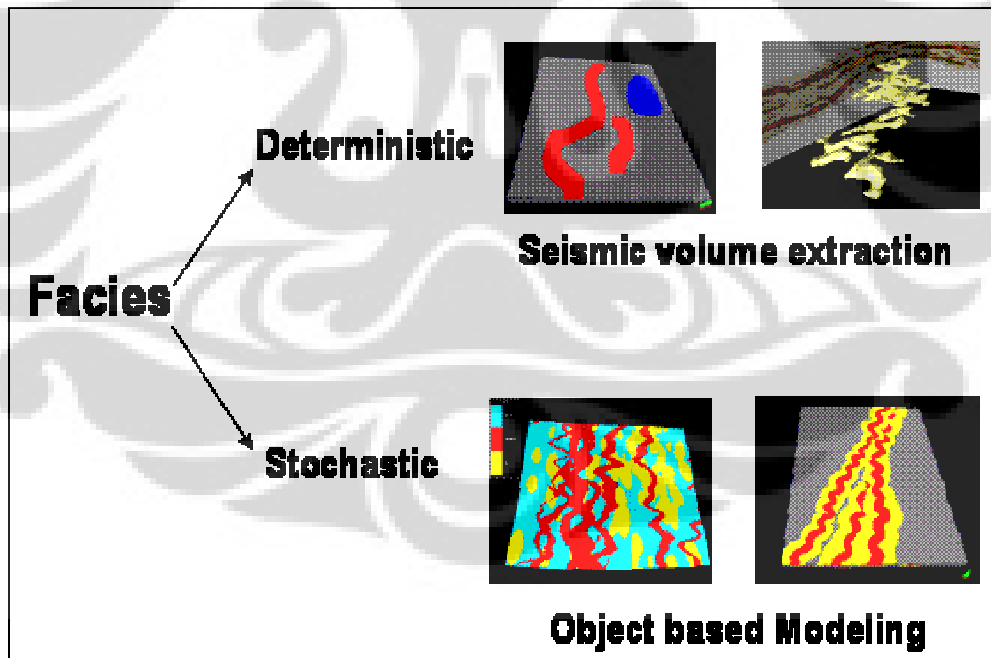


Figure 3.5 Facies determination can be simplified into two main categories: deterministic and stochastic method.

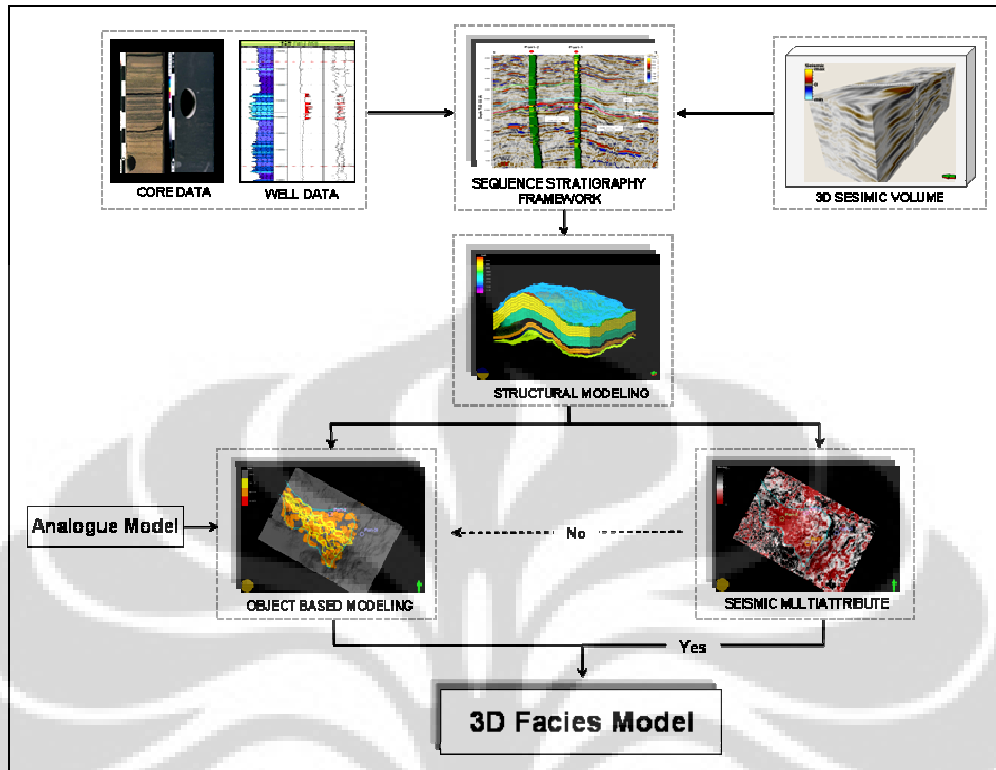


Figure 3.6 Thesis work flow

## **Chapter 4**

### **Application to Real Datasets: a Cased Study of Pari field, Kutai Basin, Offshore East Kalimantan, Indonesia**

Pari field is located in Kutai Basin, Makassar Strait, offshore East Kalimantan. The field is located in water depths range of 3,500 to 5,500 feet (1,070 to 1,680 m) and is the largest of several deepwater discoveries made in the Makassar Strait since the mid 1990s. Pari field is located in the Ganal production sharing contract (PSC) area, which Chevron and partner ENI acquired in 1997. The initial discovery well and three subsequent appraisal wells were drilled between year 2000 and 2002. The field is not yet on production. Pari field occurs where upper Miocene sands drape over an anticline. The Pari anticlinorium is one of many compressional features located in the Kutai deep water and is a gentle, low relief with northeast southwest trending. The largest reservoir in the field occurs in Upper Miocene age and was penetrated by the Pari wells at a depth of approximately 10,200 feet (3,109 m) subsea depth. Later in this thesis work, the main reservoir named as "X" reservoir unit. The "X" reservoir unit is the focus of this thesis work for reservoir characterization and facies modeling. Four wells penetrated to the "X" reservoir unit and two of them have conventional core data.

#### **4.1 Core Data Analysis**

Conventional cores data were taken from Pari-2 and Pari-5 wells to understand the sedimentology and the reservoir characteristics in Pari field. Cores from both wells were recovered the main reservoir interval with good data quality. Core data describes according to lithology, grain size,

sedimentary structures, color, amount of organics, sand bed thickness, and fossil content. Sedimentology analysis was done by Art Seller (Chevron internal report in 2000).

#### **4.1.1 Core Description from Pari-2 Well**

Core data from Pari-2 well taken at measured depths of 10,280 to 10,602 feet. Core data was intersected the "X" reservoir unit and can be divided into four main lithologic units: upper shale (10,275-10,367 feet), sand with interbedded shale (10,367-10,453 feet), lower shale (10,453-10,482 feet), and interbedded thin sand with shale (10,482-10,602 feet). Below is detail description for each stratigraphic unit.

##### Upper shale (10,275-10,367 feet)

The top part of core data (10,275-10,367 feet) is dominated with calcareous gray shale with wavy bedded to burrowed, calcareous grains include scattered echinoderm fragments, small shell and coral fragments (Figure 4.1). Small benthic and planktonic forams are locally abundant. Scattered fragments of coaly material are also present. The presence of coral fragments and distorted bedding suggest that these are transgressive or highstand deposits, many of which may have come down in slumps. This interval probably represents hemipelagic deposition during a transgression of sea level (Transgressive Systems Tract/TST).

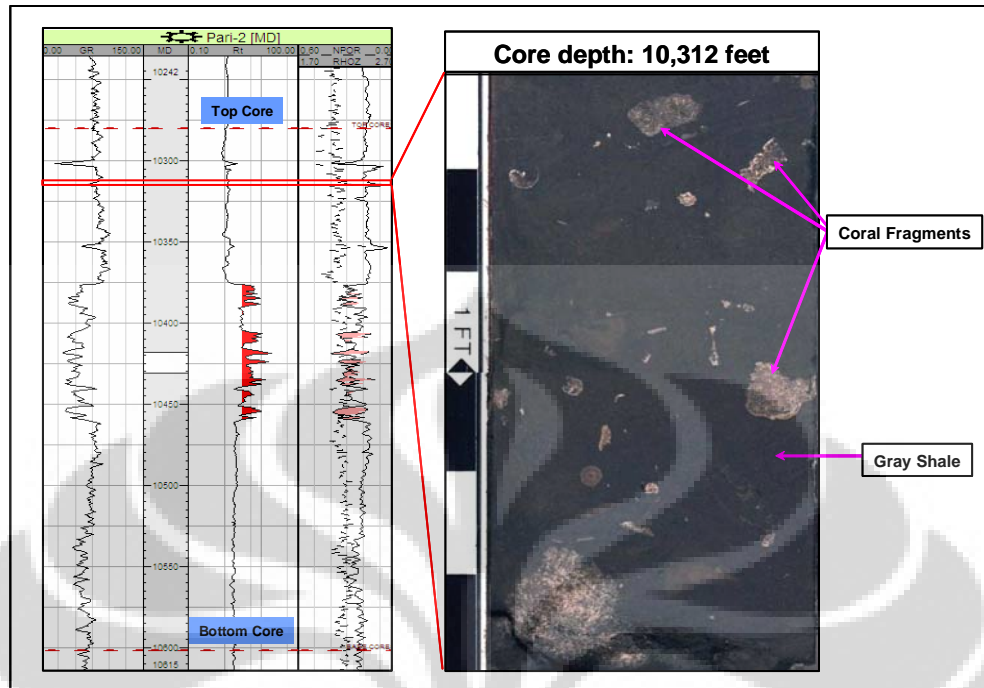


Figure 4.1 Representative log response and core photograph from Pari-2 Well. The core photograph illustrates the gray shale with coral fragments.

#### Sand with interbedded shale (10,367-10,453 feet)

This interval (10,367-10,453 feet) consists of interbedded light brown sand and gray shale. Thicker sands (10-70 cm) are generally fine-grained sand and moderately to poorly sorted. Thinner bedded sands (<6 cm thick) are usually very-fine grained and poorly sorted. Sedimentary structure in this interval describes as parallel lamination, ripple cross stratification, massive sands and burrowed structure. Horizontally laminated parts of sand beds are commonly capped by ripples and/or ripple cross-stratification (Figure 4.3). Shale-clast conglomerates occurred locally. Organic material is common in the sands and occurs as thin sheet-like pieces (leaves?). Organic material is sometimes concentrated in layers and is sometimes scattered chaotically within sand beds. These sands are interpreted as sheet sands deposited on distal lobes of submarine fans during Lowstand of sea level (Lowstand System Tract/LST).

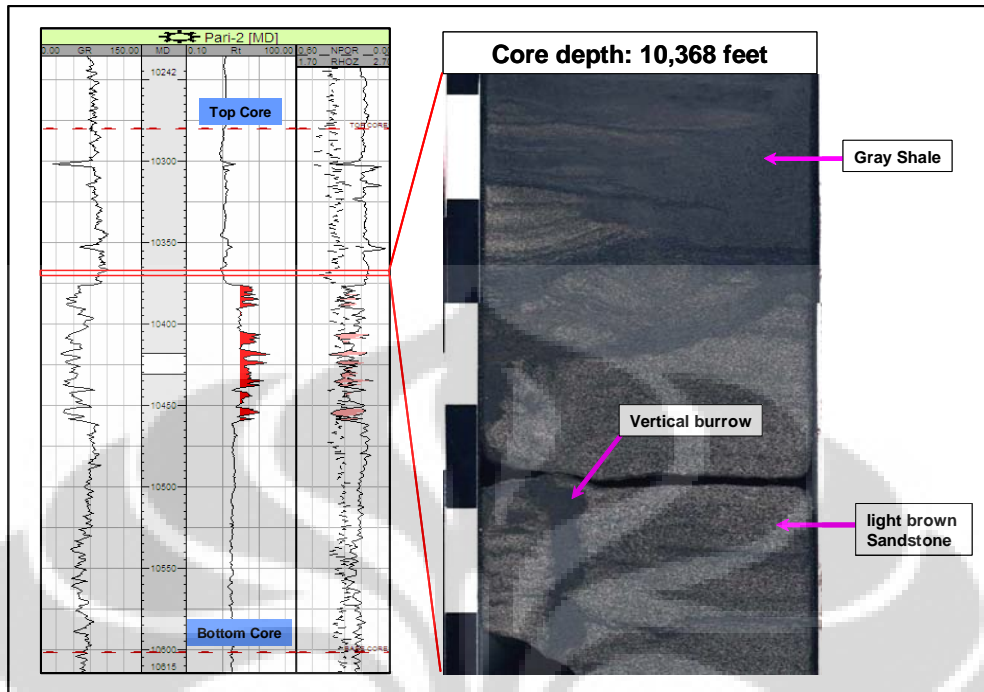


Figure 4.2 Representative log response and core photograph from Pari-2 Well. The core photograph illustrates vertical burrow on near top of sandstone overlain with gray shale.

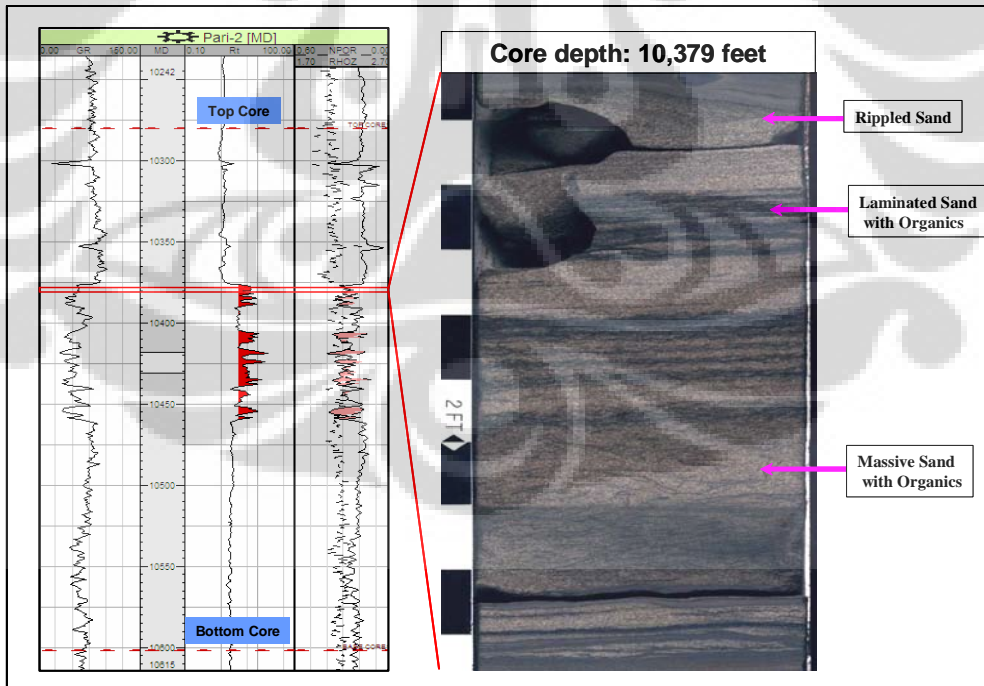


Figure 4.3 Representative log response and core photograph from Pari-2 Well. The core photograph illustrates interbedded light brown sandstone with gray shale with organic material and rippled cross stratification.

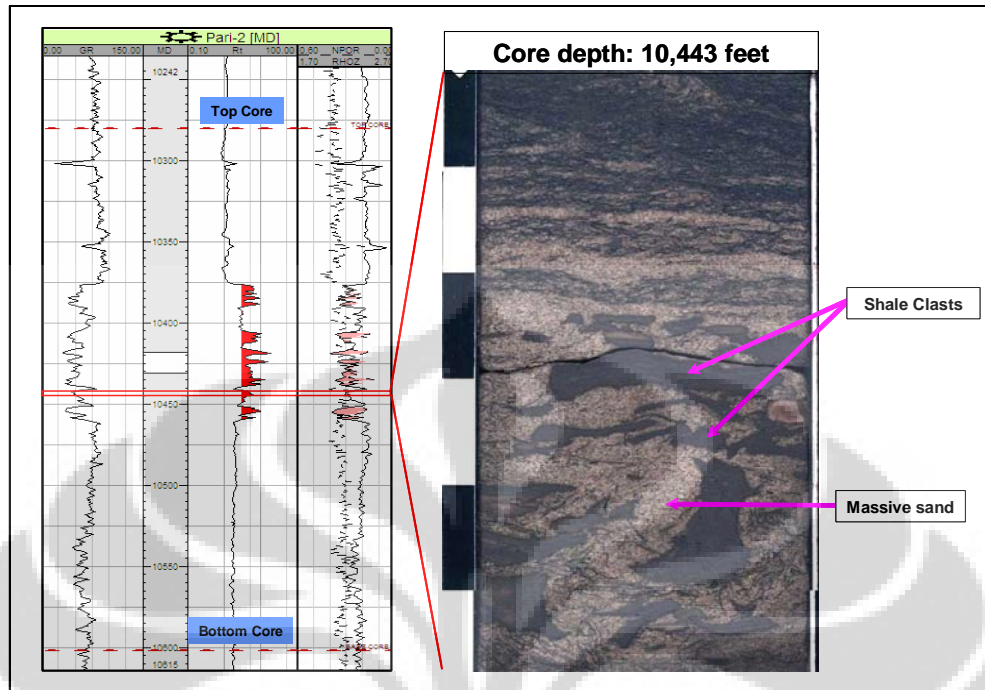


Figure 4.4 Representative log response and core photograph from Pari-2 Well. The core photograph illustrates massive sandstone with shale clast conglomerates.

Lower shale (10,453-10,482 feet)

The lower shale is dominated with gray shale, scattered irregular sand laminae and lenses. Burrows and wavy bedding are common, and locally the shale is disrupted and slumped (Figure 4.5). This could be a highstand, largely hemipelagic deposit, or could represent lowstand deposition at times when submarine fans were in different locations.



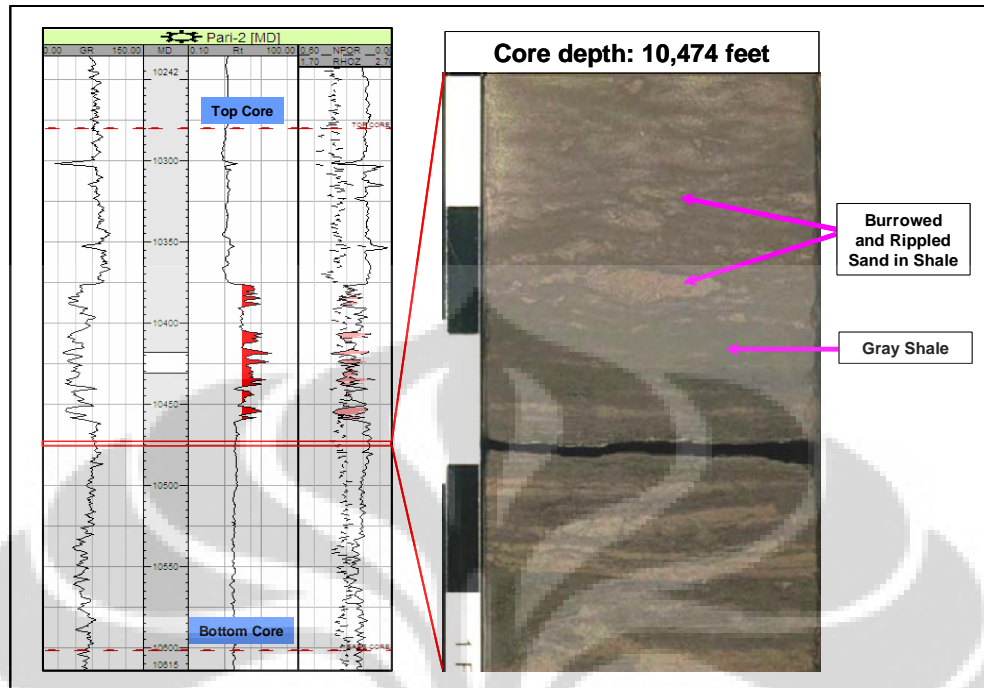


Figure 4.5 Representative log response and core photograph from Pari-2 Well. The core photograph illustrates burrowed and rippled sand in shale.

Interbedded thin sand with shale (10,482-10,602 feet)

This interval (10,482-10,602 feet) consists of interbedded light brown sand and gray shale. Sand beds are commonly 5-30 cm thick. Many sand beds fine upward from fine to very fine sand. Lower and middle parts of thicker sand beds typically have horizontal laminations. Ripples and ripple cross stratification commonly occur in the upper part of sand beds (Figure 4.6). Thinner beds are generally rippled. "Leafy" organics are associated with the sands. Shales are laminated. Shale-clast conglomerates occur locally. These sands are interpreted as sheet sands on the more distal part of a submarine fans lobe formed during Lowstand of sea level (Lowstand System Tract/LST).

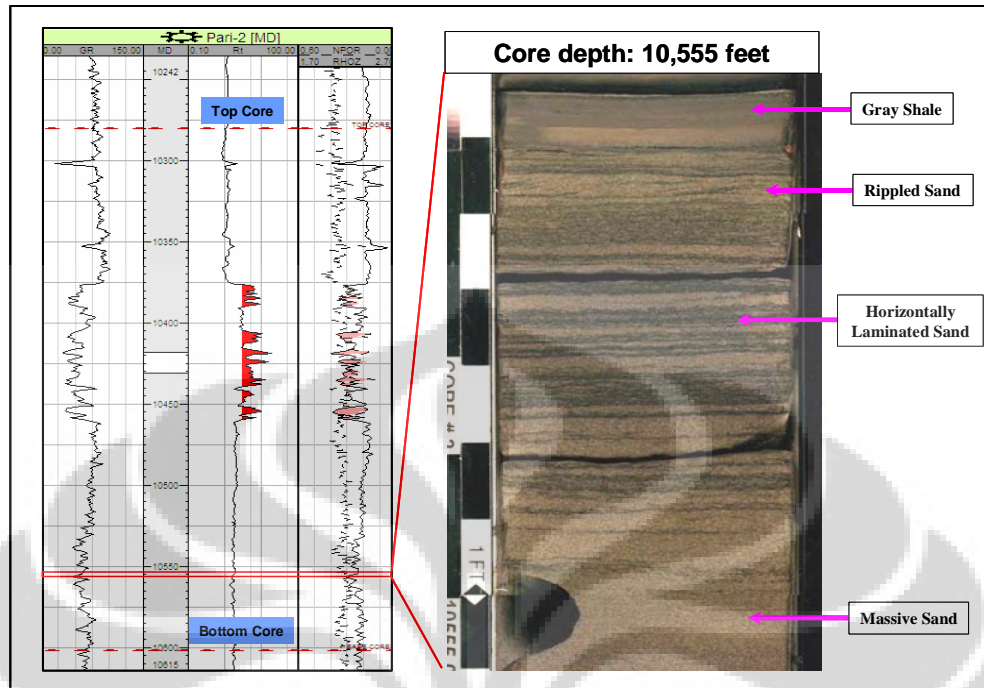


Figure 4.6 Representative log response and core photograph from Pari-2 Well. The core photograph illustrates light brown sand with massive structure in lower part, horizontal lamination and rippled structure.

#### 4.1.2 Core Description from Pari-5 Well

Core data from Pari-5 well taken at measured depths of 10,280 to 10,462.5 feet. Core data was intersected the “X” reservoir unit and can be divided into three main lithologic units: bioturbated shale (10,280-10,325 feet), shale with thin sand beds (10,325-10,403.5 feet), and sand with interbedded shale (10,403.5-10,462.5 feet). Below is detail description for each stratigraphic unit.

##### Bioturbated shale (10,280-10,325 feet)

In this interval dominated by gray shale with mottling probably related to burrowing and near surface grazers. Calcareous material (mainly small grains) is common and includes many small forams, both benthics and planktonics. This bioturbated interval has a burrowed contact with the underlying shale with thin sand beds unit (Figure 4.7). This interval

probably represents hemipelagic deposition during a transgression of sea level (Transgressive Systems Tract/TST) when in this well area was away from active turbidite flows.

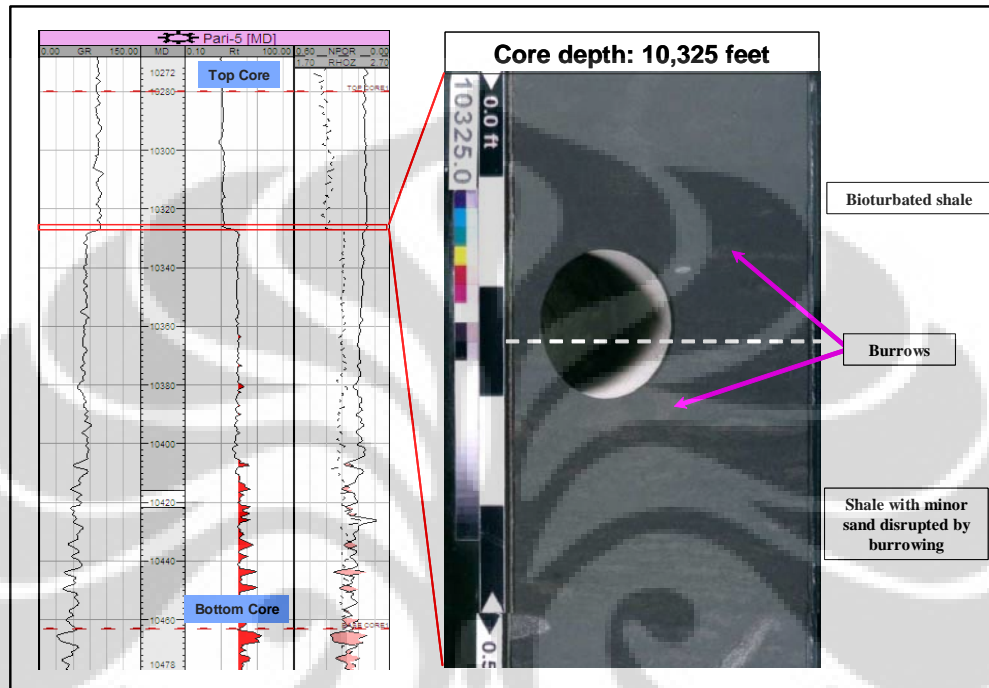


Figure 4.7 Representative log response and core photograph from Pari-5 Well. The core photograph illustrates bioturbated shale has a burrowed contact with the underlying unit (shale with thin sand beds).

#### Shale with thin sand beds (10,325-10,403.5 feet)

Shale with thin sand beds dominates in this interval. The shale is light gray and silty with burrows and bioturbation (Figure 4.8). Most sands are light brown and generally very fine-grained with clay, although a few beds are coarser and better sorted (fine-grained sand with little clay). Sand occurs as thin beds, discontinuous laminae and ripples. Starved ripples are very common. Carbonaceous material is mainly sand and silt-sized particles, and occurs in sands and shales. Carbonaceous laminae (fossil leaves?) commonly occur in lower part. Current laminated sands in burrowed shale suggest episodic currents with rapid sand deposition alternating with

slower shale deposition. This interval probably represents overbank/ levee deposition adjacent to a channel.

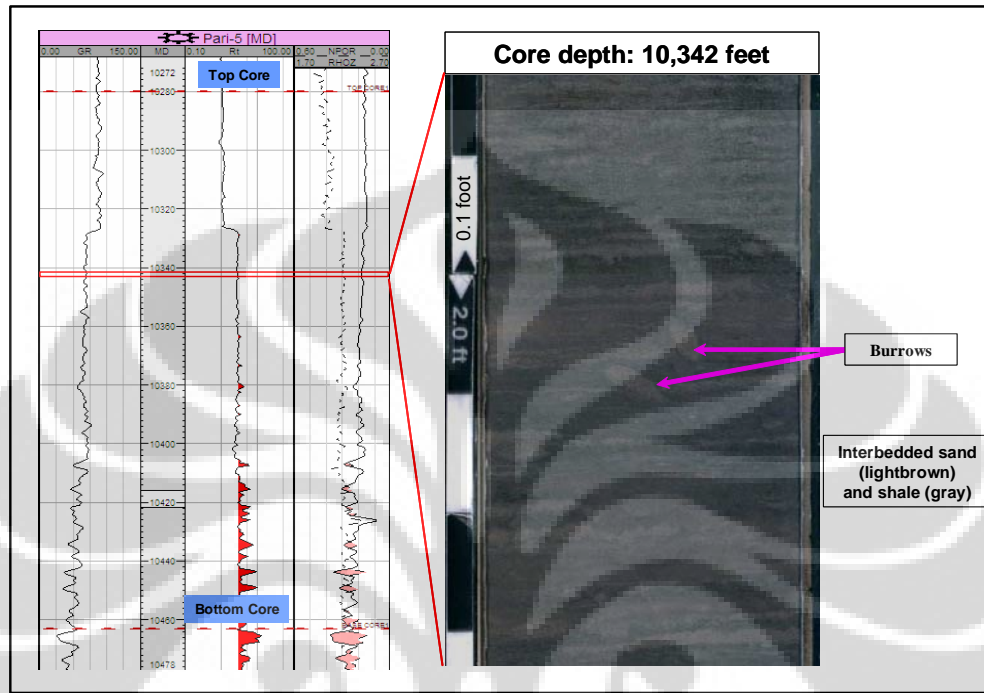


Figure 4.8 Representative log response and core photograph from Pari-5 Well. The core photograph illustrates interbedded light brown sand and gray shale with burrows structure.

#### Sand with interbedded shale (10,403.5-10,462.5 feet)

Light brown sand interbedded with medium brown shale is present in this interval. The sand is dominantly fine-grained, and many beds fine upward from upper fine to lower fine. Sand beds are highly variable in thickness, <1 to 45 cm, and bed thickness decreases slightly upward. Sedimentary structures are related to sand bed thickness. Sand beds <2 cm thick are dominated by isolated laminae and ripples. Sand beds that are 4-10 cm thick commonly have horizontal and ripple stratification (Figure 4.9). Sand beds have sharp bases, and fairly sharp tops. Amalgamated sand beds and mud clasts are rare. The lower part of this core is very similar to the lower part of core data in Pari-2 well which appears to represent turbidite deposition on submarine fan lobes. Deposition on submarine fan lobes is

further suggested by: (1) thin sand beds that are very similar in widely separated wells (Pari-2 well and Pari-5 well), (2) some moderately well sorted sands supporting deposition in the distal part of a turbidite flow after substantial transport and sorting, (3) lack of thick sands characteristic of channels, and (4) too many massive to horizontally laminated sands of moderate thickness (10-50 cm) to be a levee environment. Highly variable bed thicknesses could be related to variable turbidite flow size, multiple contemporaneous channels, and/ or multiple sources causing a single location to be in several different fans. These sands are interpreted as sheet sands deposited on distal lobes of submarine fans during Lowstand of sea level (Lowstand System Tract/LST).

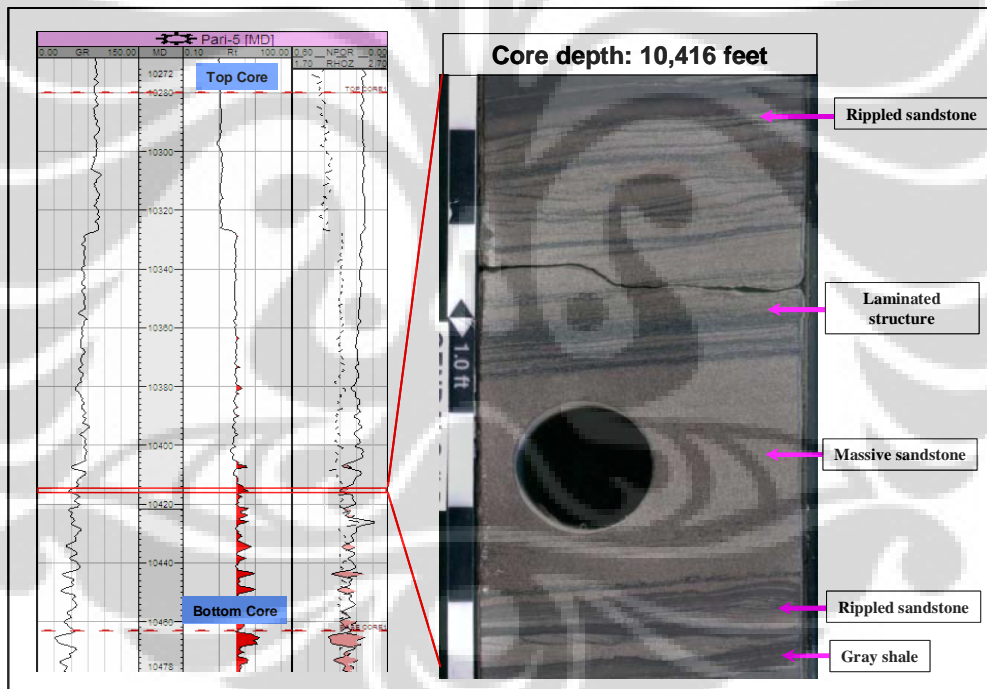


Figure 4.9 Representative log response and core photograph from Pari-5 Well. The core photograph illustrates light brown fine grained sand with dark gray shale. Laminated structure in sand is mainly fossil leaves.

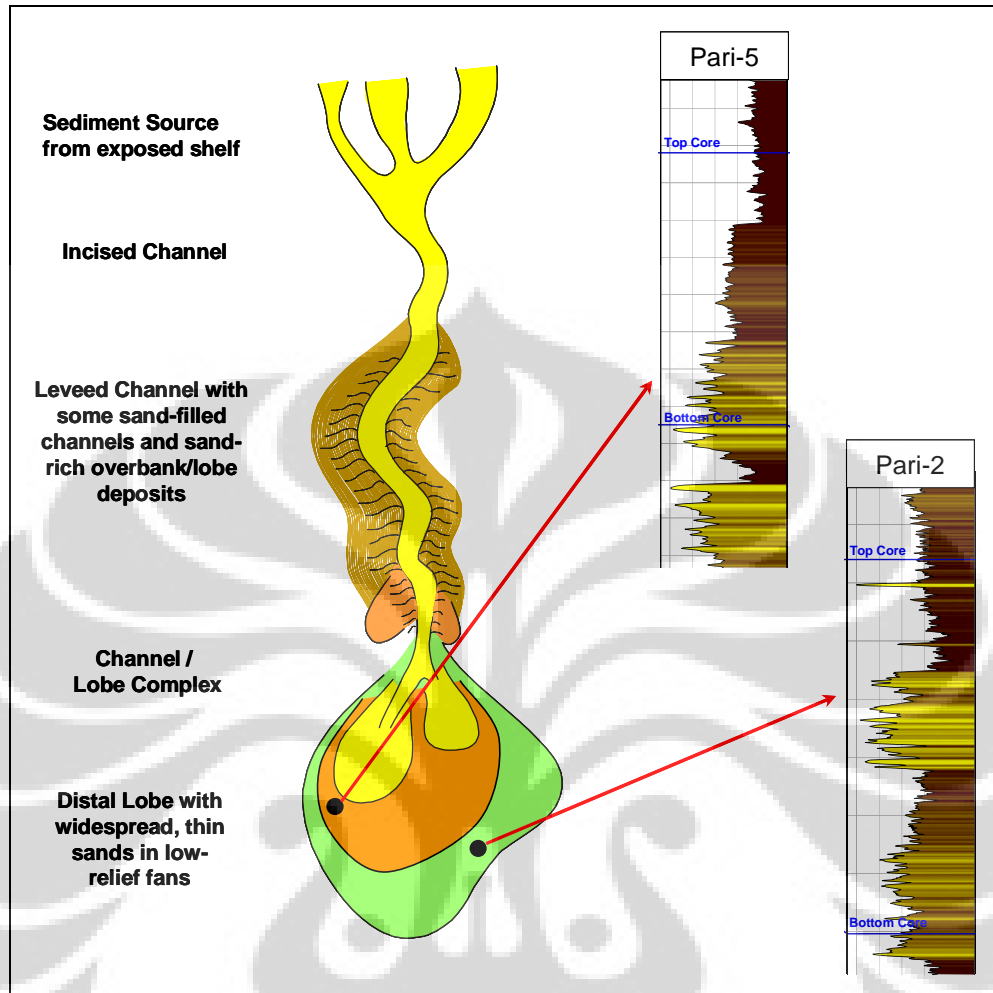


Figure 4.10 Interpreted depositional facies in general based on conventional core data in Pari-2 and Pari-5 wells within "X" reservoir unit.

## 4.2 Sequence Stratigraphy Framework of Pari Field

A generalized procedure for sequence stratigraphic framework interpretation from seismic and well data was established in study area to describe the stratigraphic evolution of the main "X" reservoir unit in Pari Field. Generalized steps in the procedure include: integrated well data and seismic data, recognition of seismic configuration and sequence boundary, and well to well correlation. Seismic sequence analysis was done by subdividing the seismic section into sequences which are the seismic expression of depositional sequences – stratigraphic units of relatively

conformable, genetically related strata bounded by unconformities or their correlative conformities and analyzing the internal character within sequence to interpret the depositional environment. Seismic sequence was defined by recognizing surfaces of discontinuity from reflection terminations in the seismic section. Surfaces of discontinuity are recognized by interpreting systematic patterns of reflection termination along the surfaces, which categorized as onlap, downlap and toplap. Sequence boundaries are then extended over the study area, including parts where reflections are concordant with boundaries. Complete correlation through the study area produces a three-dimensional framework of successively stratified seismic sequences, separated by surfaces of discontinuity.

Seismic reflection configuration analysis was done to interpret the environmental setting, depositional process and estimates lithology of the strata involves especially in the area with no well control. Although there is no unique relation between type of reflection configuration and specific lithology, the integration of the seismic data, well data and regional geology information affords a reasonable prediction of depositional environment and lithology. Several steps are involved in visual analysis of reflection configuration included the basic seismic information such as the relations to upper and lower sequences boundary (segment of onlap, downlap, and toplap) and the dominant type of reflection configuration (segment of parallel and sigmoid configuration). The thickness of sequence in "X" reservoir unit interval are mapped to combined with any other diagnostic seismic parameters to interpret the environmental setting, transport direction or other depositional aspect in Pari field. The major sequence boundaries were identified above and below the main "X" reservoir unit and correlated throughout the study area.

A complete sequence interval in Pari field was divided into three systems tract: lowstand systems tract (LST), transgressive systems tract (TST) and

highstand systems tract (HST). The lowstand systems tract can be subdivided into a lowstand fan (basin floor fan) and lowstand wedge, which may onlap an older slope and onlap or downlap to the basin floor. The basin floor forms during the most rapid rate of fall in relative sea level and the lowstand wedge form during lowest sea level (Vail, 1987). The log character in the lowstand systems tract of the sandstones reservoir in the Pari field is dominated by few massive thick sandstone and thin bedded sandstone in the upper part. The blocky, fining upward, and coarsening upward sequence may indicate backstepping, aggrading, or prograding submarine fan package, respectively that occur within the "X" reservoir unit. The lowstand systems tract associated with high-amplitude and continuous-sub continuous seismic reflections over the study area. The seismic reflection configuration of the lowstand system tract indicates a mounded external feature with sigmoid and bidirectional downlap reflection. It's interpreted as a submarine fan depositional system.

The transgressive systems tract is recognized by onlap onto older sediment and become thinner into the basin ward below. Its well log signatures consist of shale with thin bedded sandstone. The transgressive systems tract form during the rapid rate of rise of relative sea level. The highstand systems tract is deposited during a maximum high stand of sea level. The highstand parasequence in a basinal position are largely a nonporous and nonproductive zone because the lithology within this systems tract composed of silt to mud size siliciclastics. The highstand systems tract is associated with low-amplitude and continuous-sub continuous seismic reflections through the study area.



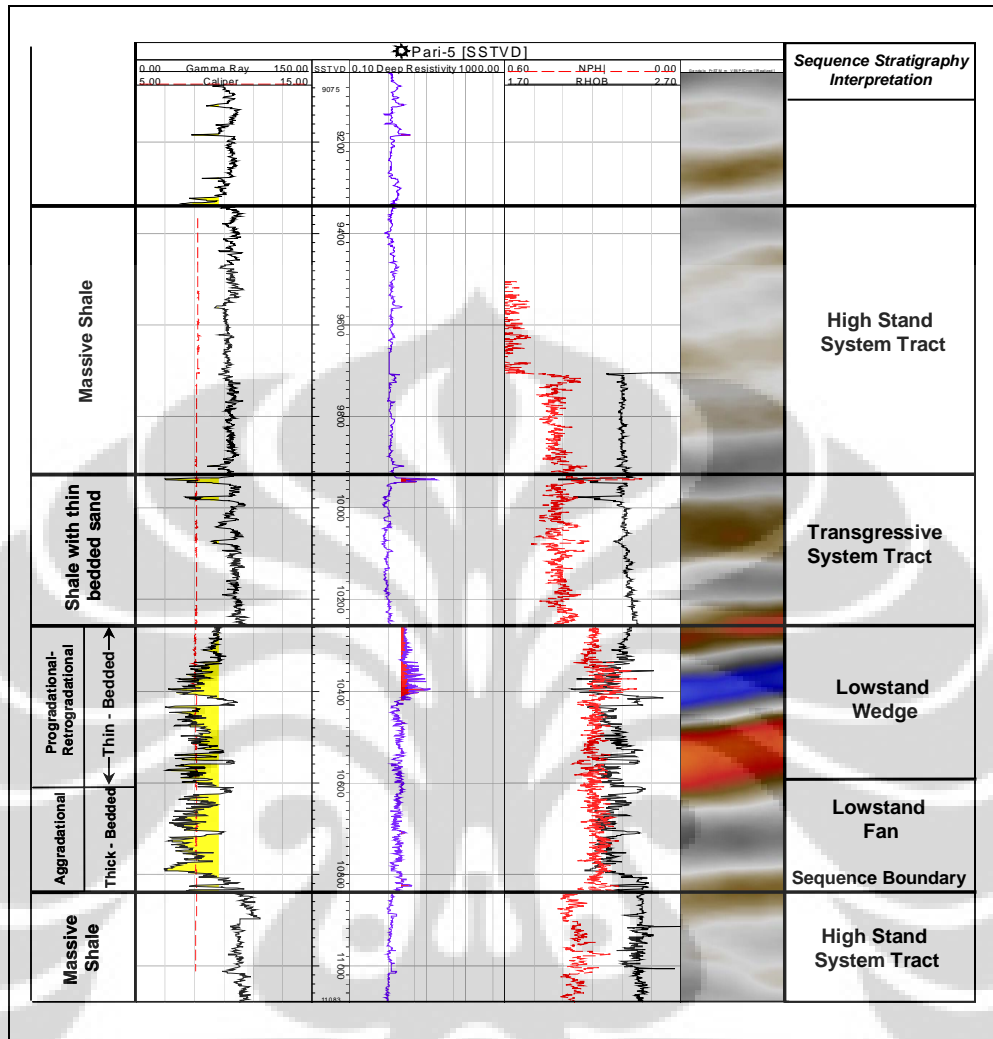


Figure 4.11 Type log in Pari-5 well illustrates the well log expression of the systems tract and seismic reflection display across Pari-5 well. The systems tract consists of lowstand systems tract (LST), transgressive systems tract (TST) and highstand systems tract (HST) with each systems tract shows specific well log expression and seismic reflection.

The seismic facies within "X" reservoir unit interval interpreted as a slope-basin floor submarine fan facies. The reflection pattern of the slope-basin floor fan facies is dominated by sigmoid and mounded external feature in the distal direction of submarine fan. This pattern is interpreted as a submarine fan deposited with medium to high depositional energy. To the proximal direction the reflection pattern is dominated with parallel-sub parallel pattern interpreted as a strata deposited in deep marine basin floor

fan of low depositional energy in the proximal area of submarine fan. The seismic facies interpretation is match with sedimentology analysis from conventional core data in Pari-2 and Pari-5 wells.

The 3D seismic data was used to correlate the reservoir unit and the systems tract within the wells due to well data has lacks of markers that can be used to correlate within the wells. So the reservoir architecture was determined largely based on seismic stratigraphy interpretation.

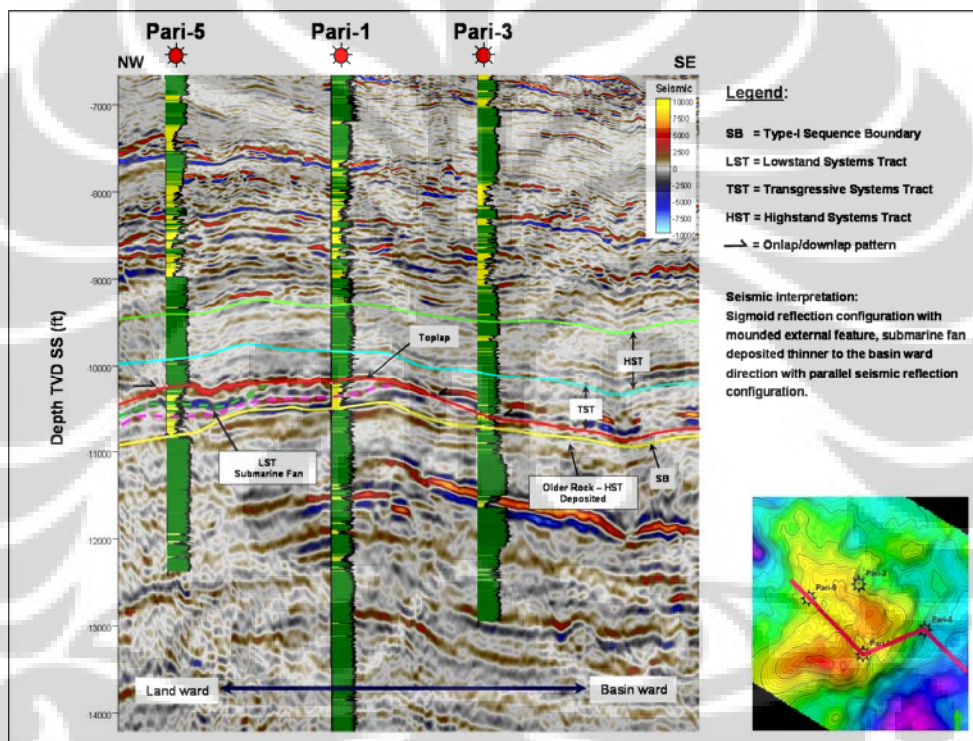


Figure 4.12 Interpreted seismic section northwest-southeast direction along submarine fan systems across Pari-5, Pari-1 and Pari-3 wells.

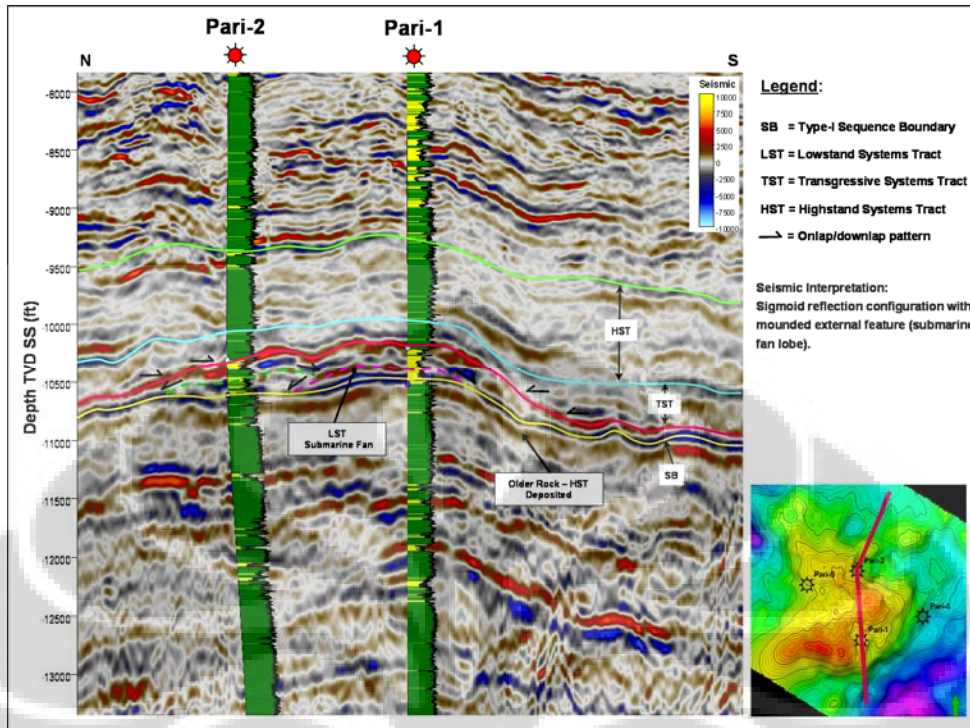


Figure 4.13 Interpreted seismic section north-south direction crossing the submarine fan systems across Pari-2 and Pari-1 wells.

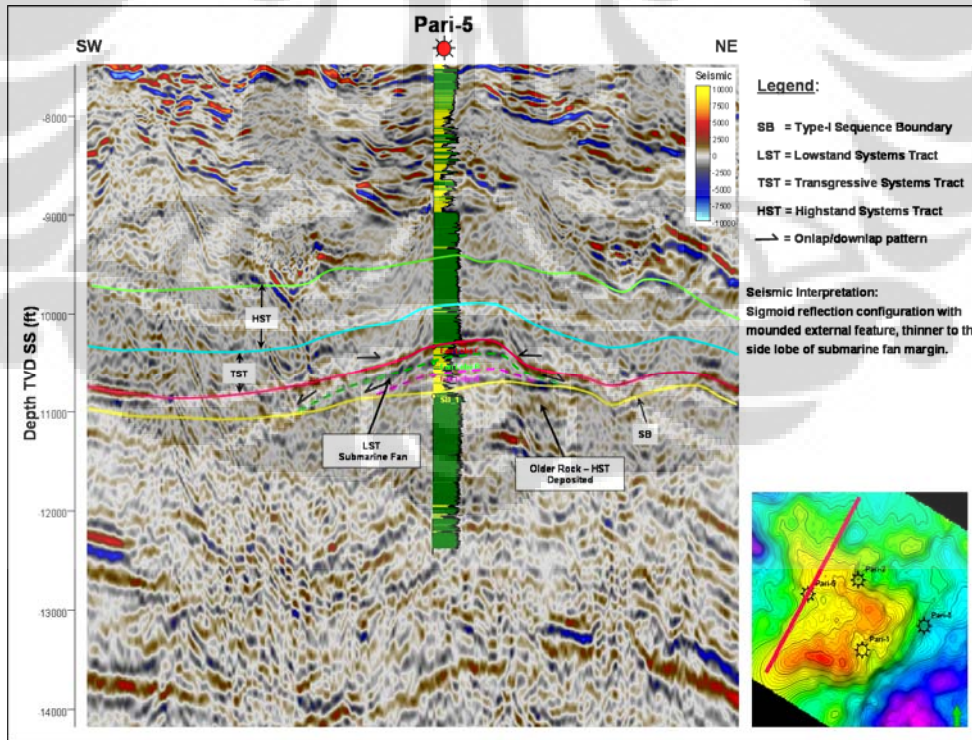


Figure 4.14 Interpreted seismic section southwest-northeast direction crossing the submarine fan systems across Pari-5 well.

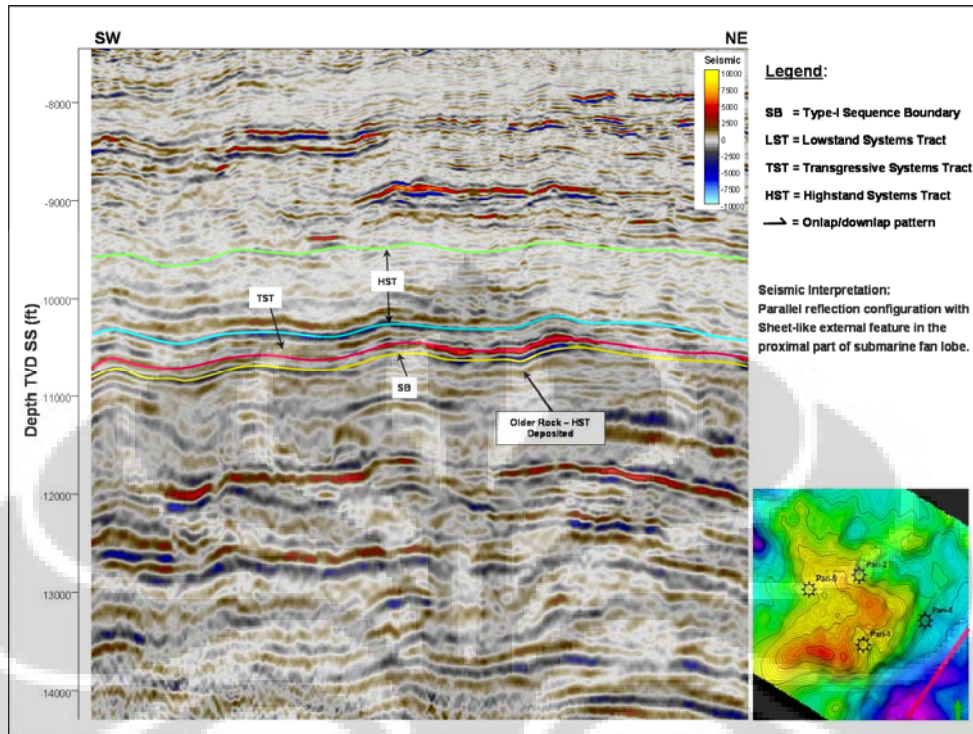


Figure 4.15 Interpreted seismic section southwest-northeast direction in the proximal part of submarine fan systems.

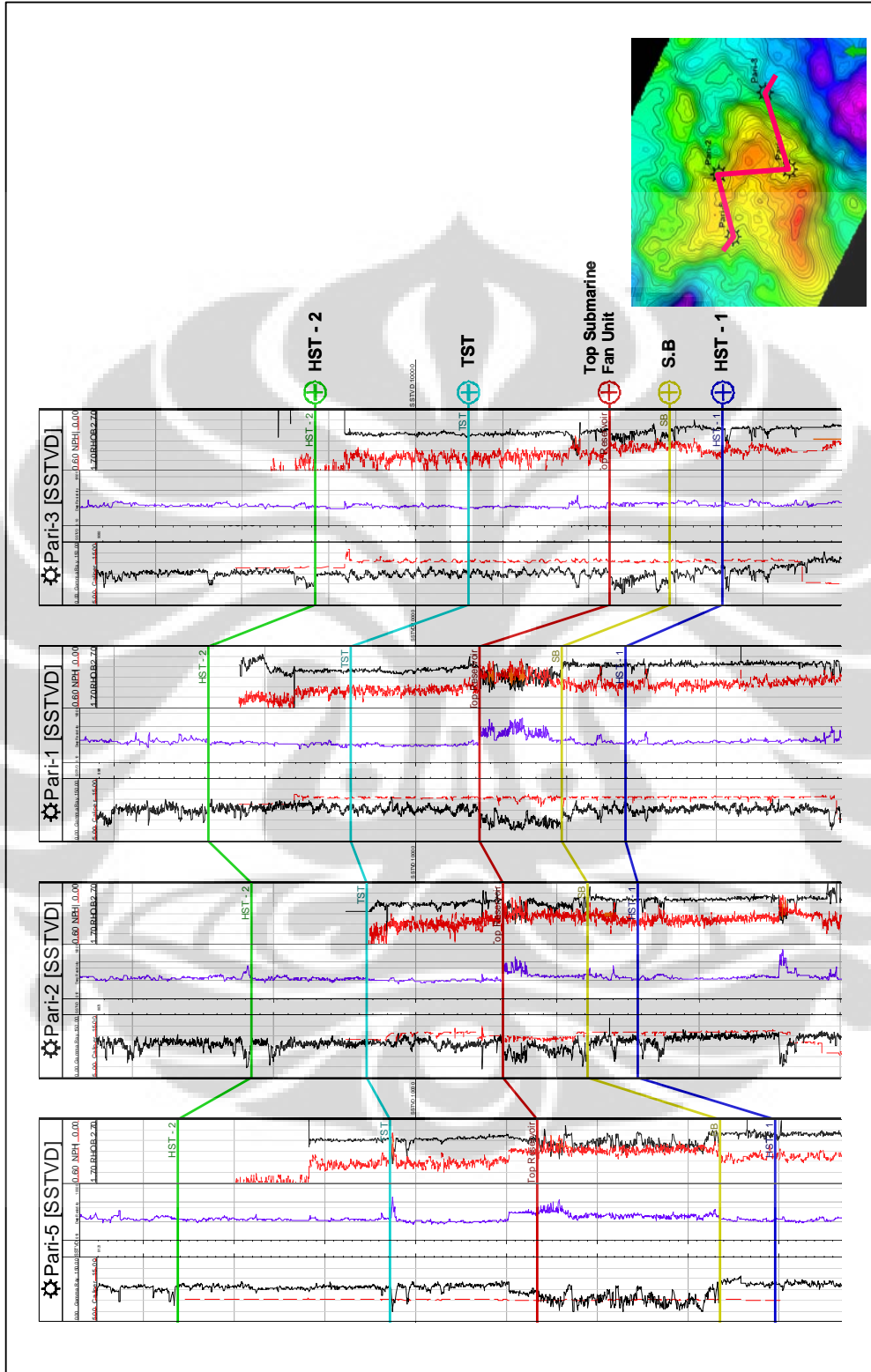


Figure 4.16 Structural correlation section across Pari-5, Pari-2, Pari-1 and Pari-3 showing the well markers of the interpreted systems tracts.

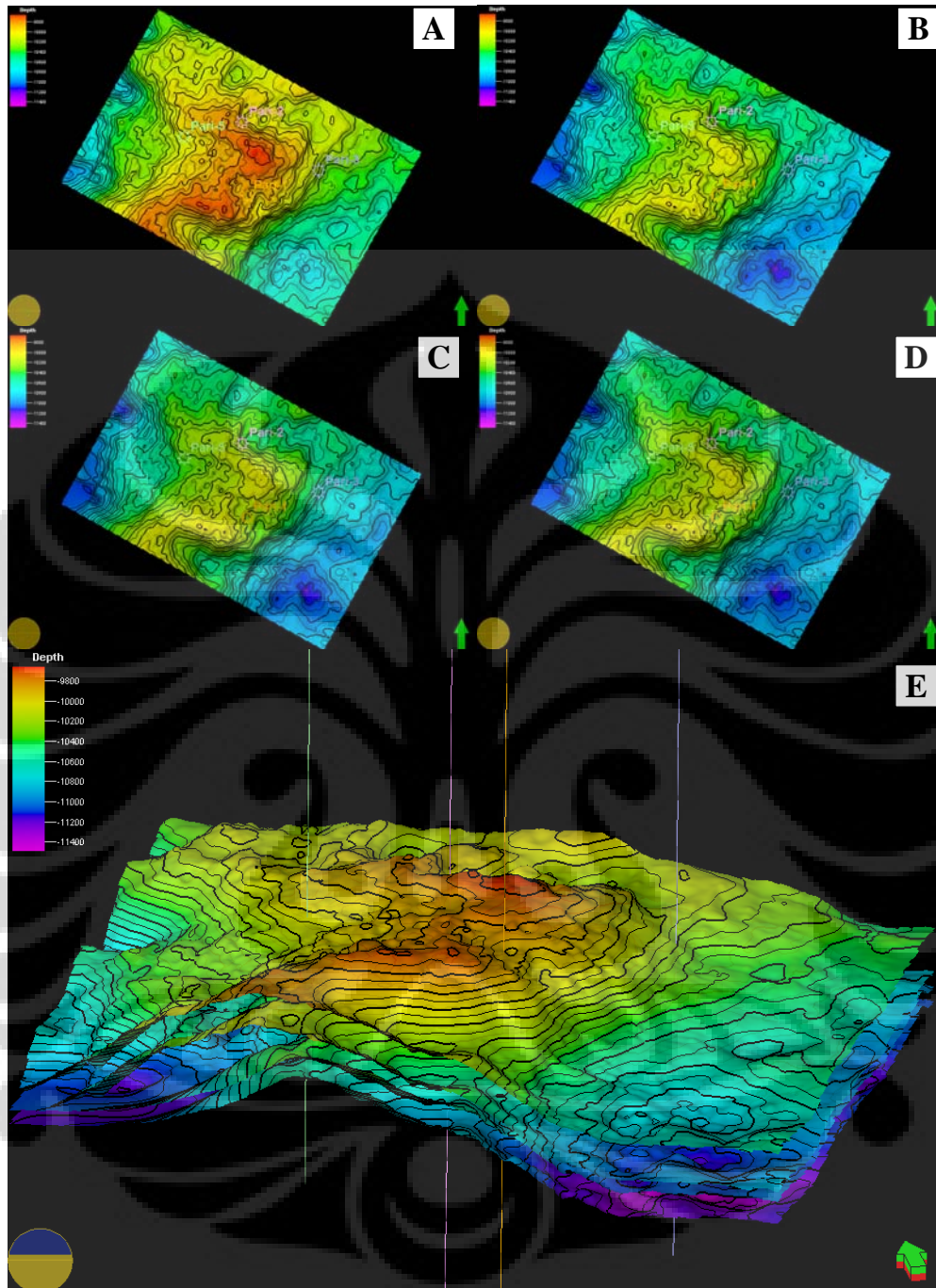


Figure 4.17 Interpreted depth structure map on each sequence boundary over the study area (A) Top structure map on upper highstand systems tract (B) Top structure map on transgressive systems tract (C) Top structure map on lowstand systems tract (D) Top structure map on lower highstand systems tract (E) 3D view of the depth structure maps.

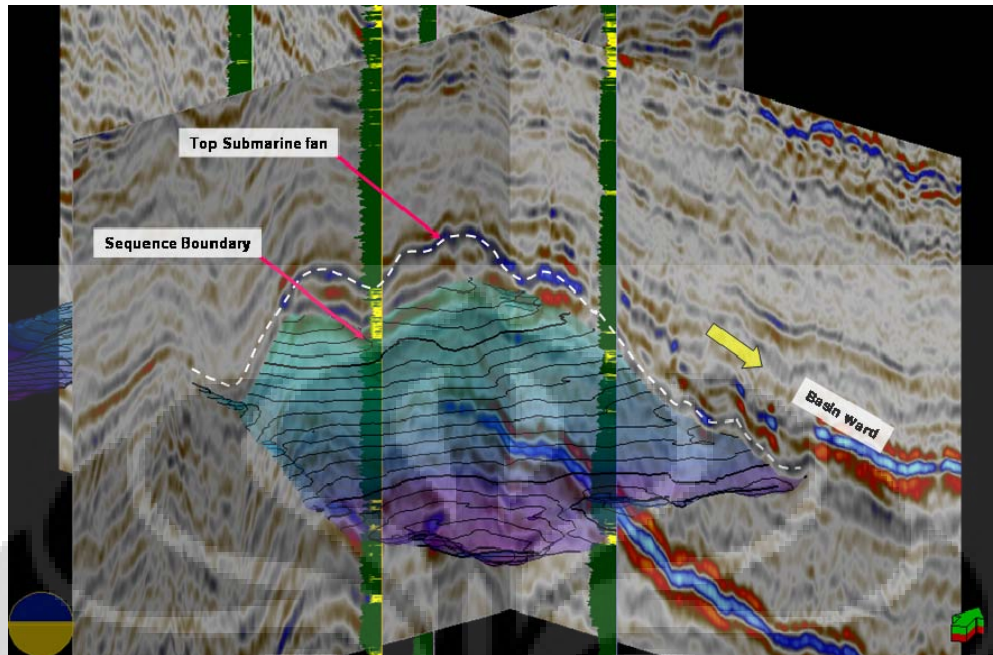


Figure 4.18 Three Dimensional (3D) view showing seismic intersection and interpreted sequence boundary of submarine fan.

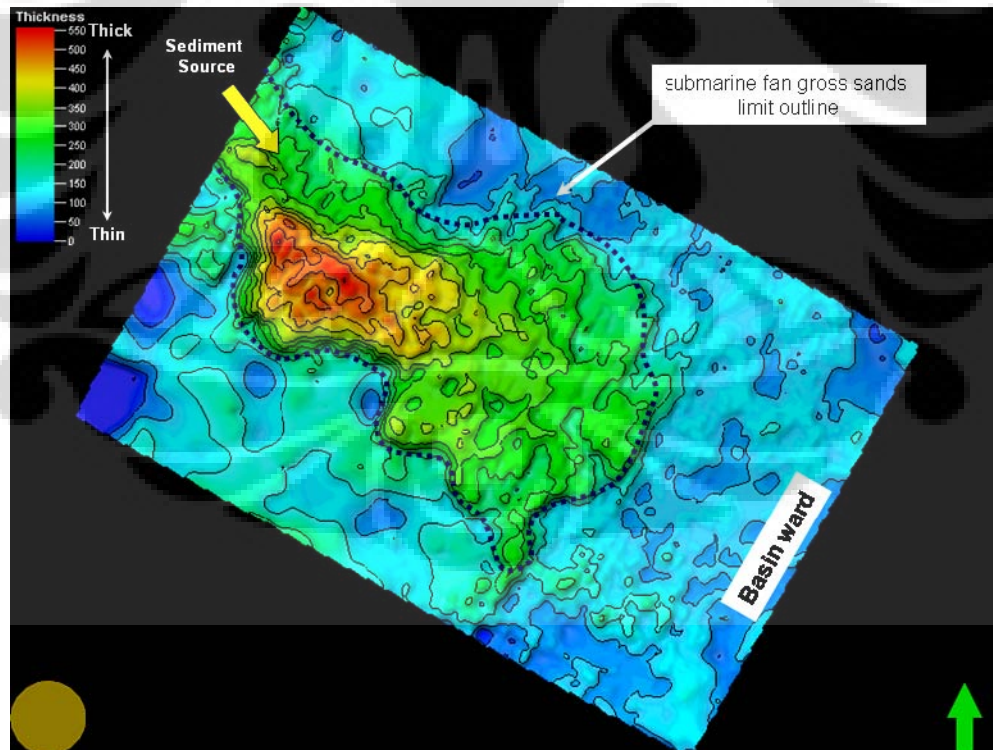


Figure 4.19 Isopach map of "X" reservoir unit showed the outer limit of submarine fan gross sands and relative sediment source from northwest direction.

### 4.3 Pari Field Structural Modeling

Static reservoir modeling for the “X” reservoir unit interval in Pari field was performed using Petrel software. The static modeling workflow started with import well and seismic data, structural modeling, well log analysis and facies modeling. Seismic interpretation using 3D seismic data over Pari field clearly illustrated large anticlinal structure with local small anticlines as main hydrocarbon trapping mechanism. The anticlines are slightly asymmetric, with the steeper limb to the east. Seismic amplitude and seismic coherency attribute (variance) was evaluated to detect any major faults in Pari field. The structural evaluation indicates no obvious major fault developed in study area. Seismic amplitude discontinuity appears to indicate small fault which consider has no significant effect in reservoir modeling. However, some structural uncertainty exist due to rugose bathymetry, hydrate effect in shallow section and water bottom multiples that effect the structural configuration within target zone.

Pillar gridding constructed to generates the 3D framework. The grid is represented by pillars (coordinate lines) that define the possible position for grid block corner points. The objective of the grid is to capture the reservoir geometry in appropriate size for reservoir simulation. The cell dimension is 50 x 50 meters (X,Y). The grid is orthogonal with vertical pillars and a N125°E orientation, which corresponds to the depositional trend of the “X” reservoir unit in Pari Field. The grid area is 76,300 acres and limited to the reservoir limits and 3D seismic data coverage. The vertical layering is parallel the top of each zone along the 3D structural grid.



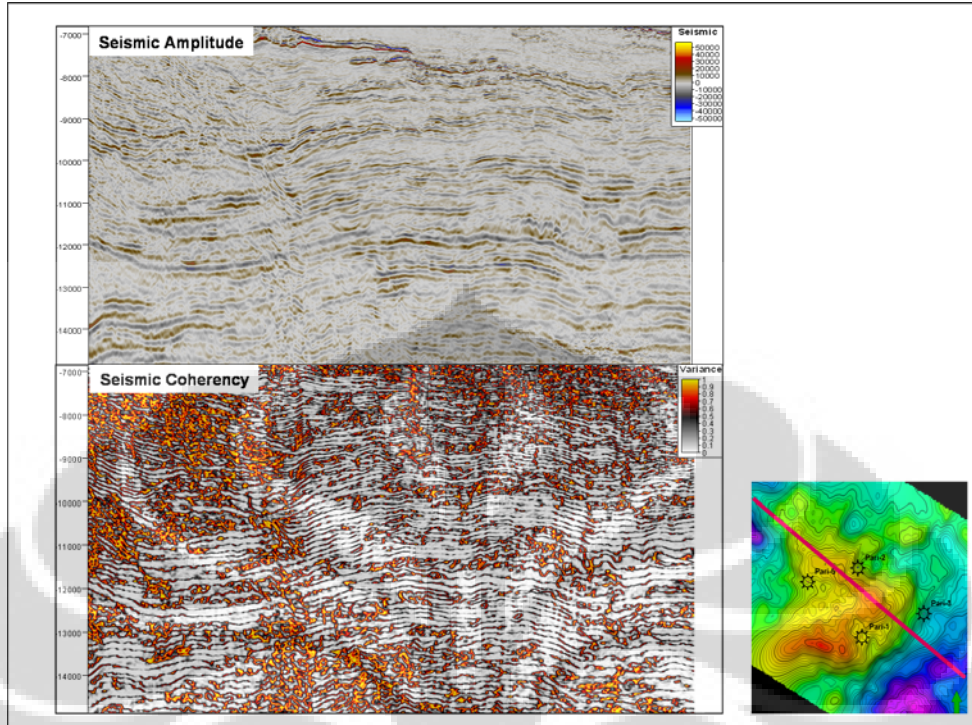


Figure 4.20 Seismic amplitude display (above) and seismic attribute coherency display (below). The seismic display indicated no obvious fault developed in Pari field. Seismic amplitude discontinuity appears to indicate small fault which consider has no significant effect in reservoir modeling.

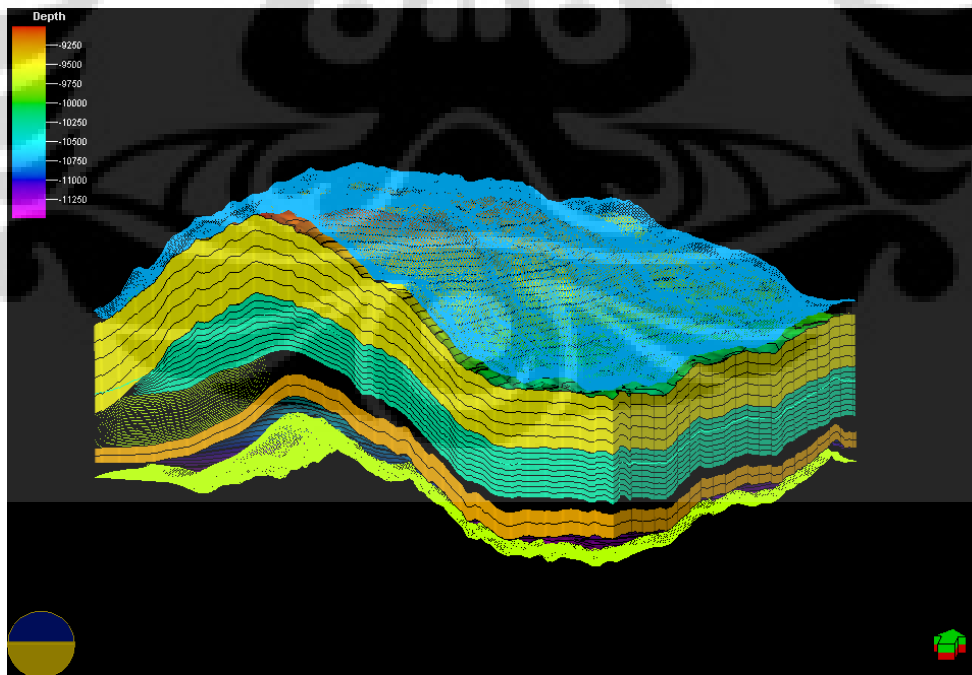


Figure 4.21 Three dimensional (3D) model showing the structural framework and layering of the main reservoir interval in the Pari field.

## 4.4 Pari Field Facies Modeling

Many oil and gas reservoirs around the world were deposited in slope and basin-floor settings as submarine fans including reservoir in Pari field. Based on outcrop data, these submarine fans are commonly composed of multiple lobes that are not resolvable on three dimensional (3D) seismic data. The internal characteristics of fan lobes, including channels and sheetlike splay lobes, are also important parts of reservoir modeling that may not be clearly imaged in seismic or well data but likely will affect fluid flow. Therefore it's important to understand the reservoir characteristics and the facies distribution to optimized hydrocarbon recovery. In this thesis work, one of the objectives is to model the facies distribution of the "X" reservoir unit using the available 3D seismic data and well data.

### 4.4.1 Well Data Analysis

Well data used to generate net to gross ratio for the main "X" reservoir unit in Pari field. The well data penetrated by the four well are interpreted as being representative of the reservoir as a whole. The wells are widely spaced 3-7 kilometers apart, penetrated different part of the submarine fan. The logged interval also has a relatively consistent in logged reading and has good log quality. Net to gross ratio calculated based on gamma ray index (GR Index) calculation for each well. Gamma ray index match with the facies description from core data. There are four group of lithofacies determined based on gamma ray index cut-off. Those lithofacies are: High net to gross (GR index cut off = 0.0 – 0.3), medium net to gross (GR index cut off = 0.3 – 0.5), low net to gross (GR index cut off = 0.5 – 0.7) and shale dominated (GR index cut off = 0.7 – 1.0). The high net to gross lithofacies associated with sand dominated. High net to gross lithofacies associated with submarine channel depositional facies. The medium net to gross lithofacies associated with subequal layers of sandstone and claystone. It's associated with sheetlike splay lobe

depositional facies. The low net to gross lithofacies contains claystone with 10- 30% sand laminae. Low net to gross lithofacies associated with channel-levee depositional facies or sheetlike splay lobe. Shale lithofacies has dominated by claystone and associated with hemipelagic depositional systems. The upscaled facies logs were obtained from the upscaled net to gross logs based on the net to gross cut-off.

Well Name	Seq. Boundary	Depth (TVDSS)	Gross Thickness (ft)
<b>Pari-1</b>	HST-1	-10,697	211
	S.B	-10,486	274
	Top Reservoir	-10,212	428
	TST	-9,784	472
	HST-2	-9,312	
<b>Pari-2</b>	HST-1	-10,786	180
	S.B	-10,606	297
	Top Reservoir	-10,309	483
	TST	-9,826	406
	HST-2	-9,420	
<b>Pari-3</b>	HST-1	-10,886	154
	S.B	-10,732	174
	Top Reservoir	-10,558	405
	TST	-10,153	443
	HST-2	-9,710	
<b>Pari-5</b>	HST-1	-10,992	153
	S.B	-10,839	504
	Top Reservoir	-10,335	405
	TST	-9,930	585
	HST-2	-9,345	

Table 4.1 Interpreted depth and gross thickness calculation for each sequence stratigraphic boundary in Pari wells.

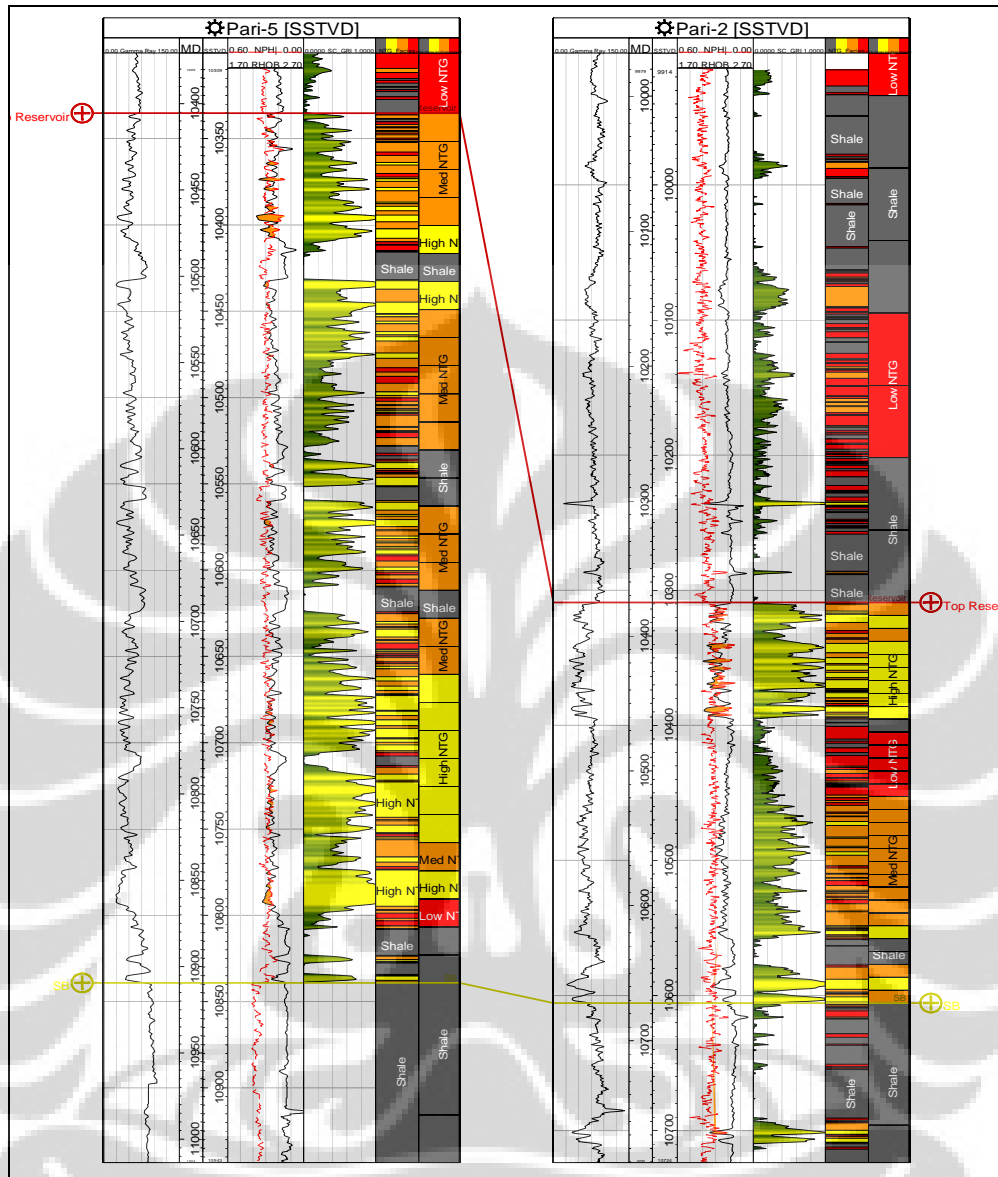


Figure 4.22 Correlation from Pari-5 to Pari-2 wells within “X” reservoir unit showing the log data (gamma ray, neutron-density) and interpreted lithofacies based on the net to gross cut-off and the final upscaled net to gross log.

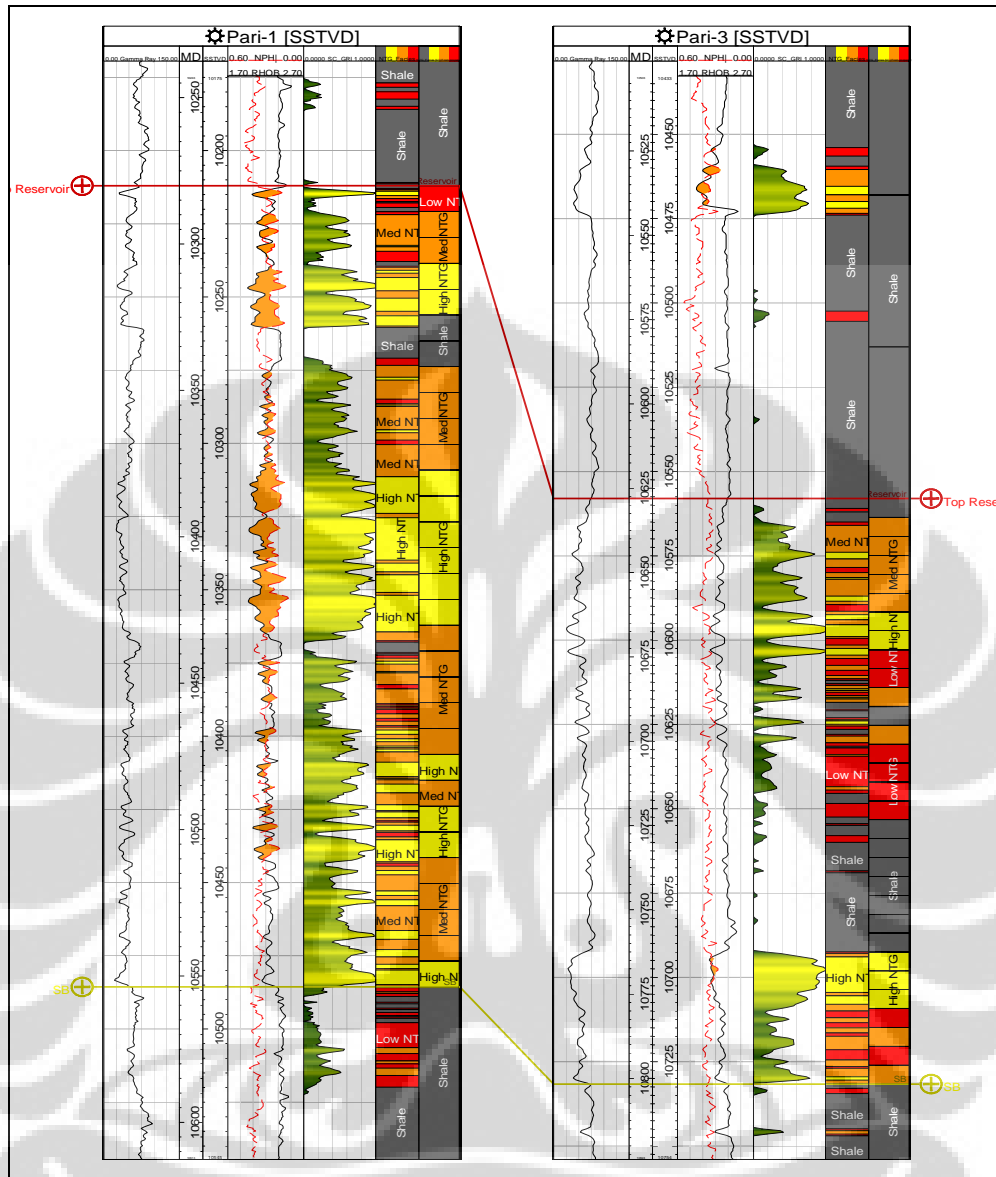


Figure 4.23 Correlation from Pari-1 to Pari-3 wells within “X” reservoir unit showing the log data (gamma ray, neutron-density) and interpreted lithofacies based on the net to gross cut-off and the final upscaled net to gross log.

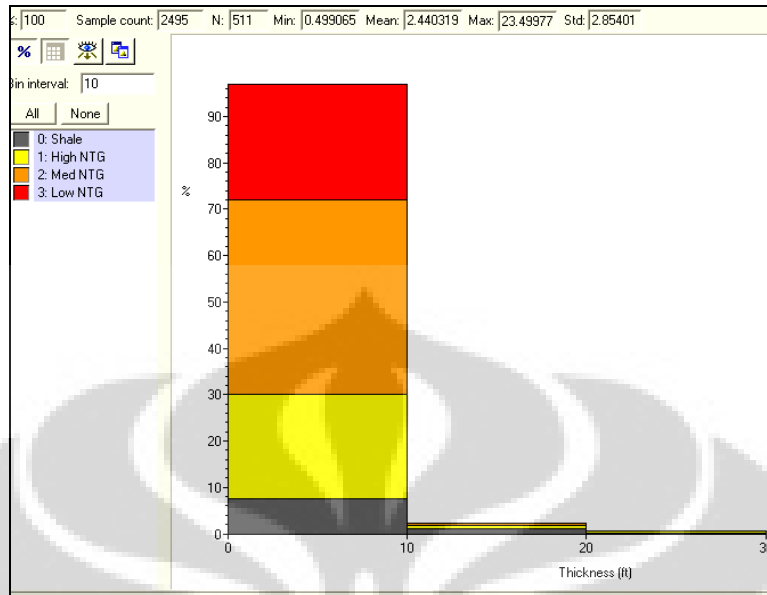


Figure 4.24 Thickness distribution for each lithofacies from Sequence Boundary (S.B) to Top of "X" reservoir unit. The dominant thickness is between 0 to 10 feet.

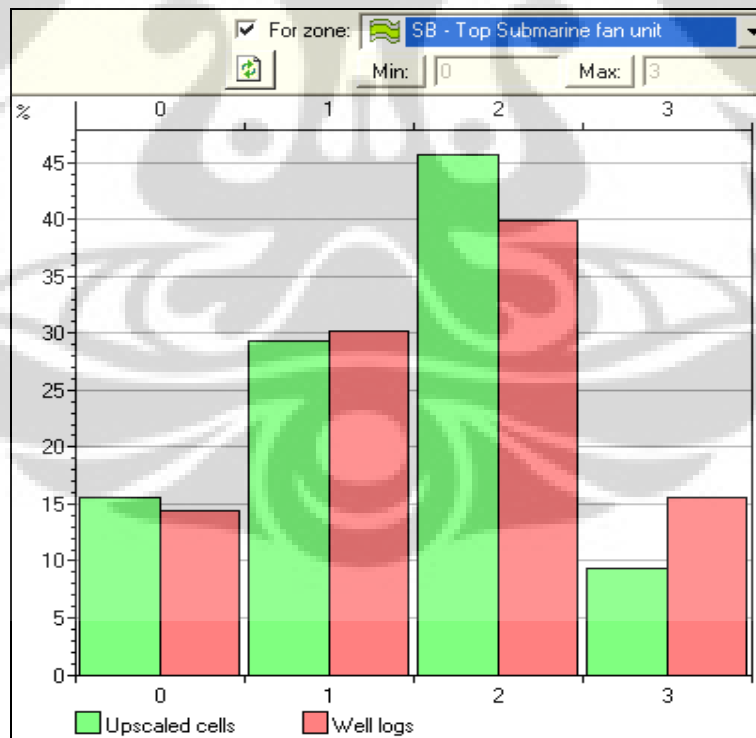


Figure 4.25 The histogram plot showing the percentage of each lithofacies for the original well logs data compare with the upscaled cells from Sequence boundary (S.B) to Top of "X" reservoir unit.

## 4.4.2 Seismic Multiattribute Analysis

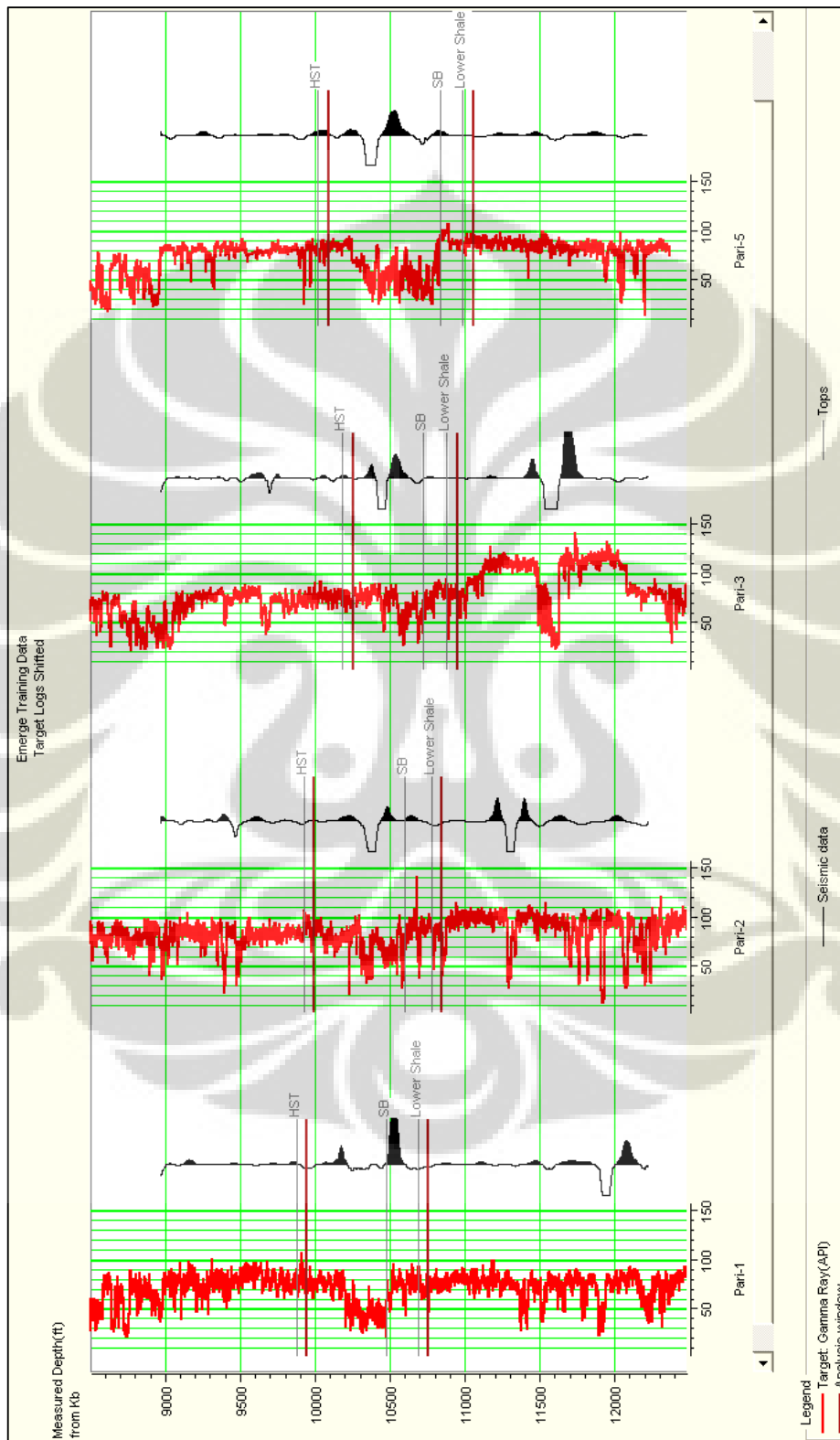


Figure 4.26 Gamma Ray log display (red curve) from Pari-1, Pari-2, Pari-3 and Pari-5 wells as a target log for multiattribute analysis using e-merge application software to identify the facies and reservoir distribution within “X” reservoir unit in Pari field.

	Target	Final Attribute	Training Error	Validation Error
1	Gamma Ray	Cosine Instantaneous Phase	16.202767	16.559929
2	Gamma Ray	Instantaneous Phase	15.621422	16.040884
3	Gamma Ray	Amplitude Envelope	15.499946	16.459838
4	Gamma Ray	Amplitude Weighted Frequency	15.325338	16.161706
5	Gamma Ray	Apparent Polarity	15.220146	16.269743
6	Gamma Ray	Filter 5/10-15/20	15.145478	16.212507
7	Gamma Ray	Integrate	15.082032	16.261616
8	Gamma Ray	Quadrature Trace	14.981206	16.459964
9	Gamma Ray	Derivative Instantaneous Amplitude	14.948103	17.043022
10	Gamma Ray	Filter 15/20-25/30	14.916077	17.045149

Figure 4.27 Final attribute analysis showing the training error and validation error for each attribute with gamma ray log as the target log.

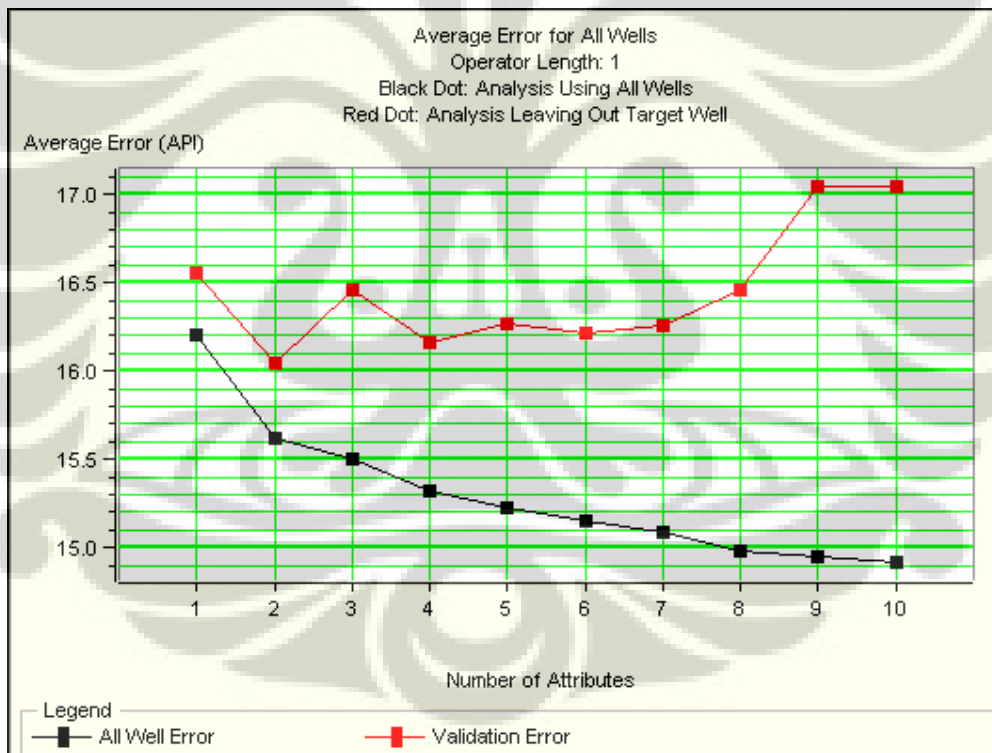


Figure 4.28 Cross plot between numbers of attributes versus average error from multiattribute analysis.



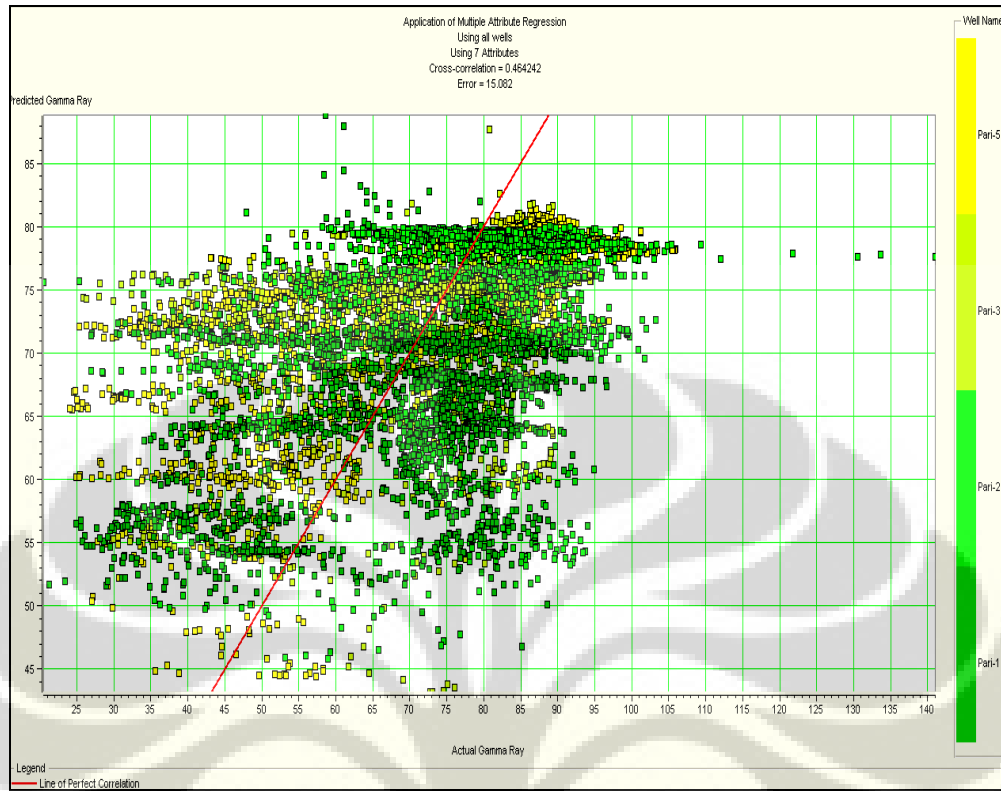


Figure 4.29 Cross plot between actual gamma ray versus predicted gamma ray using 7 attributes from all Pari wells. The cross plot showing 0.46 cross correlation.

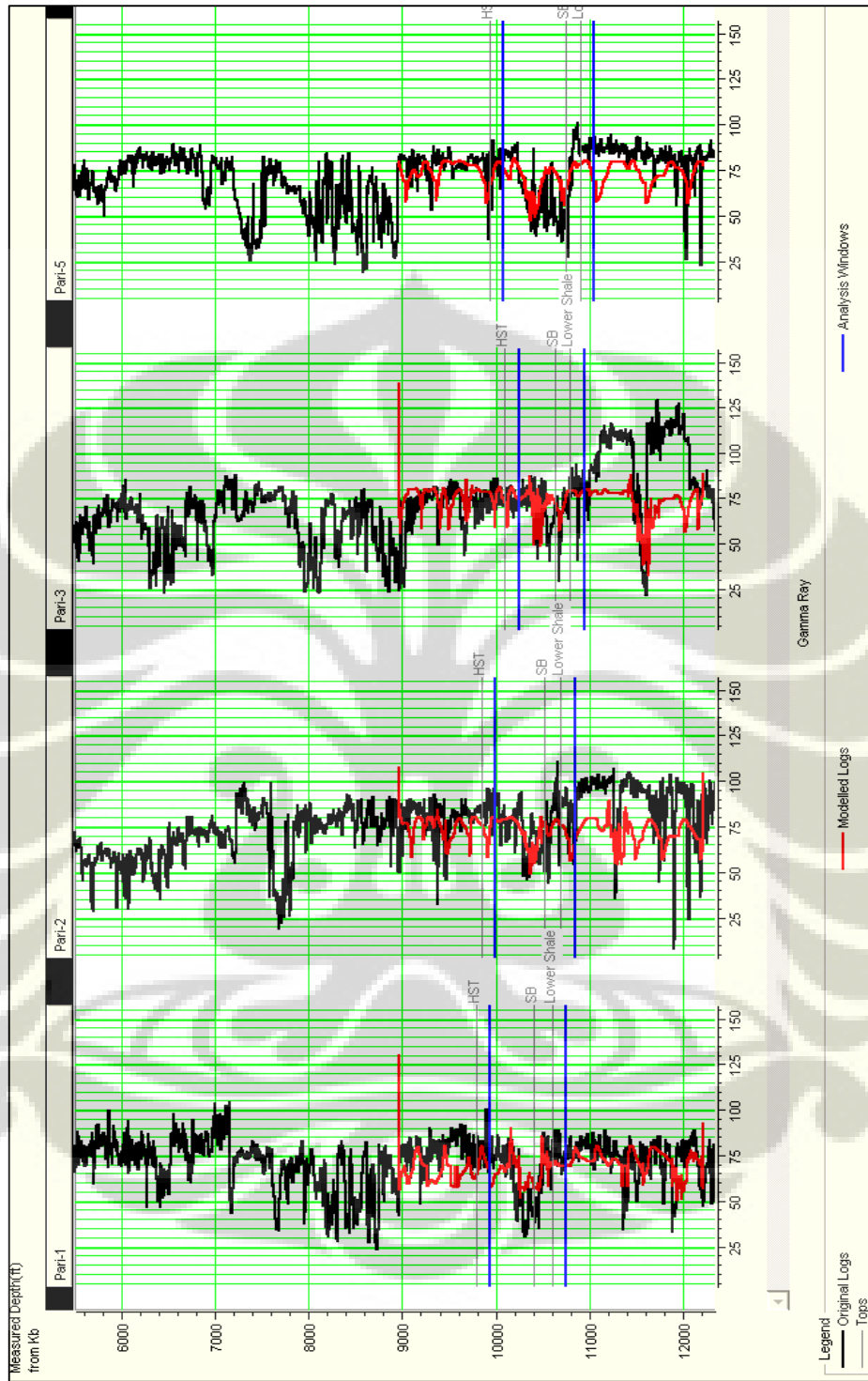


Figure 4.30 Gamma Ray log (black curve) and modeled log (red curve) from Pari-1, Pari-2, Pari-3 and Pari-5 wells from seismic multiattribute analysis using e-merge application software to identify the facies and reservoir distribution within “X” reservoir unit in Pari field.

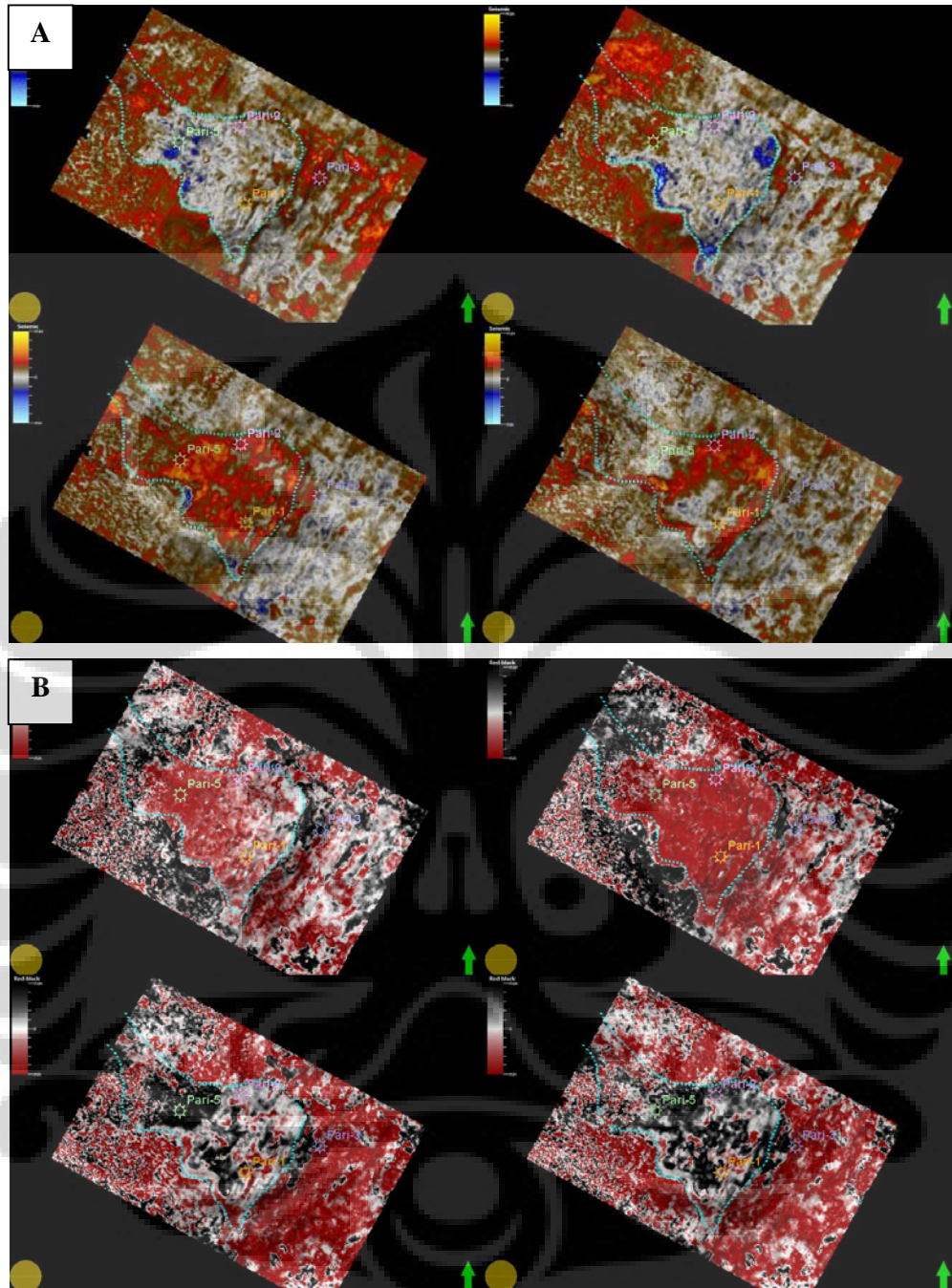


Figure 4.31 Seismic amplitude maps (A) and seismic multiattribute maps (B) indicate gross submarine fan deposited used as a reservoir boundary for object based modeling, detail internal submarine fan configuration can not be resolved due to seismic resolution.

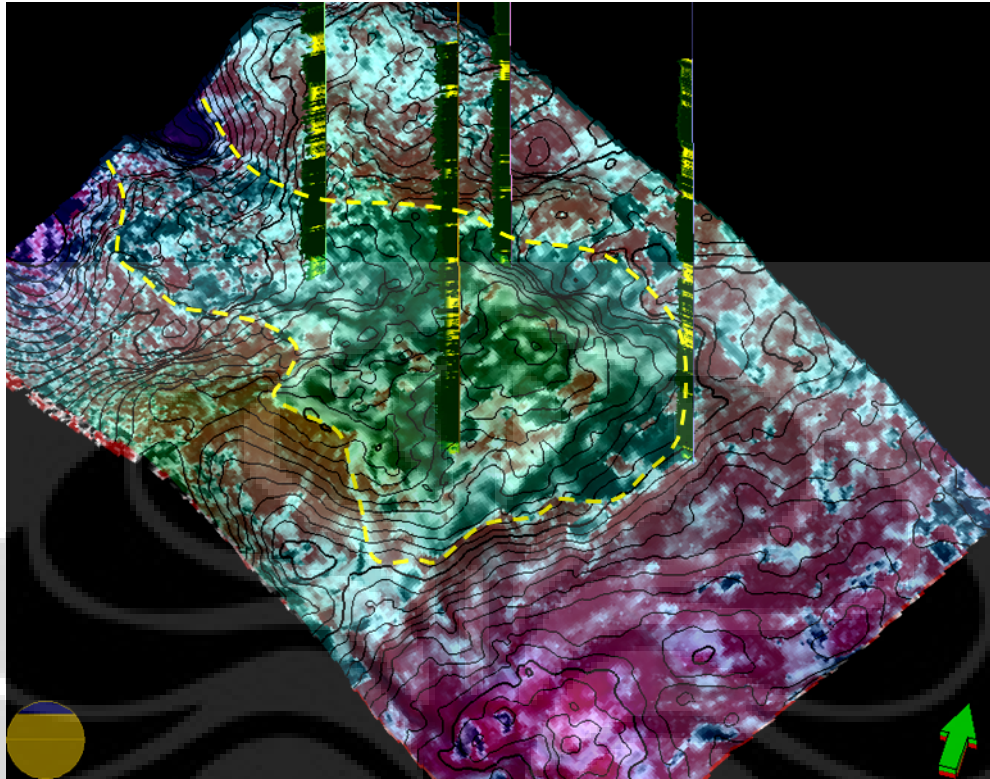


Figure 4.32 Three dimensional (3D) view showing the seismic multiattribute overlaying with structural contour of top reservoir. Pari field is a large anticline with the submarine fan reservoir drape over the structure.

#### 4.4.3 Object Based Facies Modeling

Based on the result of seismic multiattribute analysis, the internal architecture of the “X” reservoir unit in Pari field could not be resolved using the 3D seismic data and four well penetrations. The seismic multiattribute can only delineated the gross sand limit of the submarine fan. Hence, analogue is needed to characterize the internal reservoir architecture of the interpreted submarine fan. The method used to characterize the internal architecture of submarine fan within “X” reservoir unit is using an object based modeling method. The analogue used for the object based modeling is a Pleistocene submarine fan in the northern part of the study area. The study of this Pleistocene submarine fan analogue

was done by Saller et al. in 2004. Below is the detail description of the Pleistocene submarine fan analogue model.

#### **4.4.4 Submarine Fan Analogue**

In the deep water of the Kutai Basin, offshore East Kalimantan, Indonesia, a Pleistocene basin floor fan is clearly imaged in the shallow subsurface and serves as an analogue for “X” reservoir unit the Pari field. Sandy facies in both the Pleistocene analogue and the “X” reservoir unit are believed to be fine-grained turbidites sourced from shelf-edge lowstand deltas and deposited as channelized lobes in a weakly confined to unconfined setting near the base of slope. The Pleistocene fan contains many individual lobes with sheetlike splay elements and channels that can be resolved in the shallow 3-D seismic data.

The basin-floor fan is part of a lowstand system linked to a shelf-edge delta deposited during a lowstand of sea level that ended at approximately 240 ka (Saller et al., 2004). The fan is mostly basinward of a toe-thrust belt on the middle and lower slope of the northern Kutai Basin. The most basinward toe-thrust anticline that bounds the basin floor is on the western margin of the Pleistocene fan. The basin-floor fan is approximately 40 km basinward of the lowstand delta that fed it. The existing water depth in the vicinity of the basin-floor fan is approximately 2,000 m (6,700 feet). The basin-floor fan described here is approximately 22 km wide (north–south along strike) and extends at least 22 km into the basin (west to east along dip). In its thickest part, the fan is approximately 170 m (550 feet) thick. The fan is located where the sea-floor slope gradient decreases from 2.1° on the slope to 0.3° on the basin floor.

Each fan lobe is composed of many reservoir elements, some of which can be resolved on the shallow seismic data. Intralobe elements that were

studied on Pleistocene fan include sheetlike splays, distributary channels, and channels incised into older lobes. Some lobes, especially early ones, are dominated by splays, whereas others are dominated by channels. Most lobes have substantial amounts of both splay and channel elements. Although each lobe is unique, ranges and averages of element characteristics can be determined. Sheetlike Splay Elements Relatively flat (planar) continuous reflectors with relatively consistent amplitude are a common architectural element within lobes. These sheetlike splays may terminate because of truncation by erosional channels, onlap against other lobes, and/or by downlap. The geometry of sheetlike splays elements from Pleistocene submarine fan, used as an analogue for facies modeling in "X" reservoir unit in Pari field is shown on Table 4.2.

Pleistocene fan lobes also contain distributary channels. Distributary channels are straight to slightly sinuous and in general, distributary channels are more common in basinward (eastern) lobes. The tops of many older lobes were modified by slightly sinuous channels cut into underlying lobes. They fed basinward lobes and are relatively discontinuous because they are commonly cut by later channels. The geometry of channel elements from Pleistocene submarine fan, used as an analogue for facies modeling in "X" reservoir unit in Pari field is shown in Table 4.3.

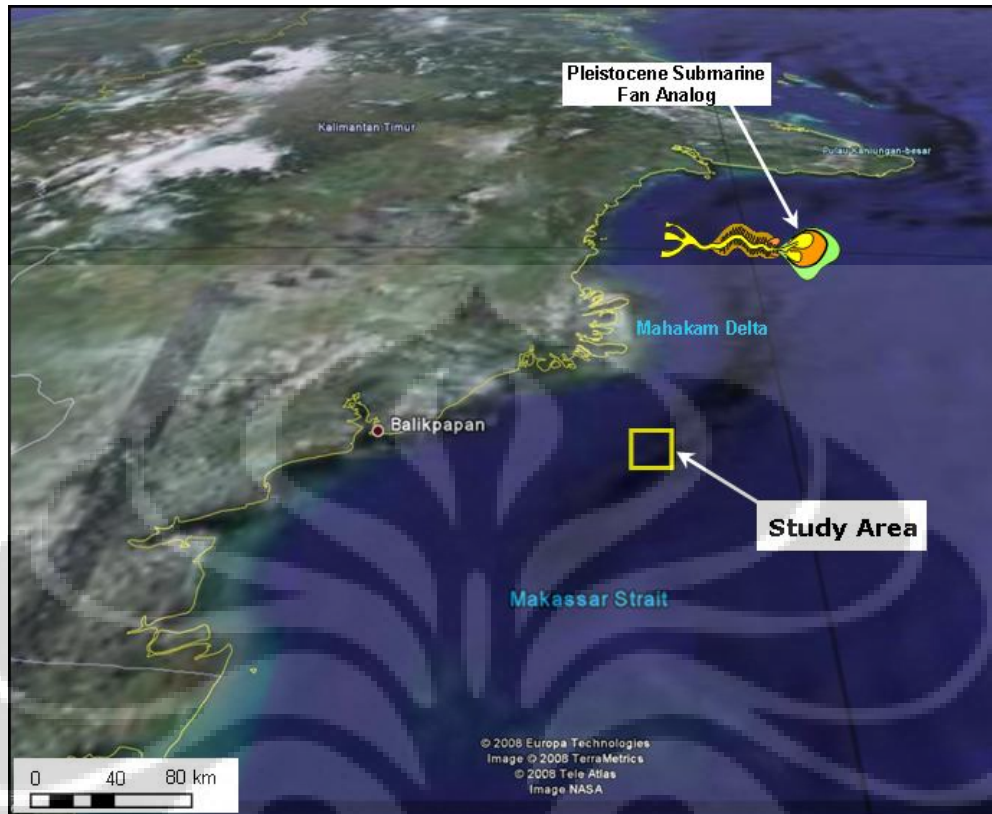


Figure 4.33 Map showing the study area and the Pleistocene submarine fan location in the northern part, offshore East Kalimantan, Indonesia.

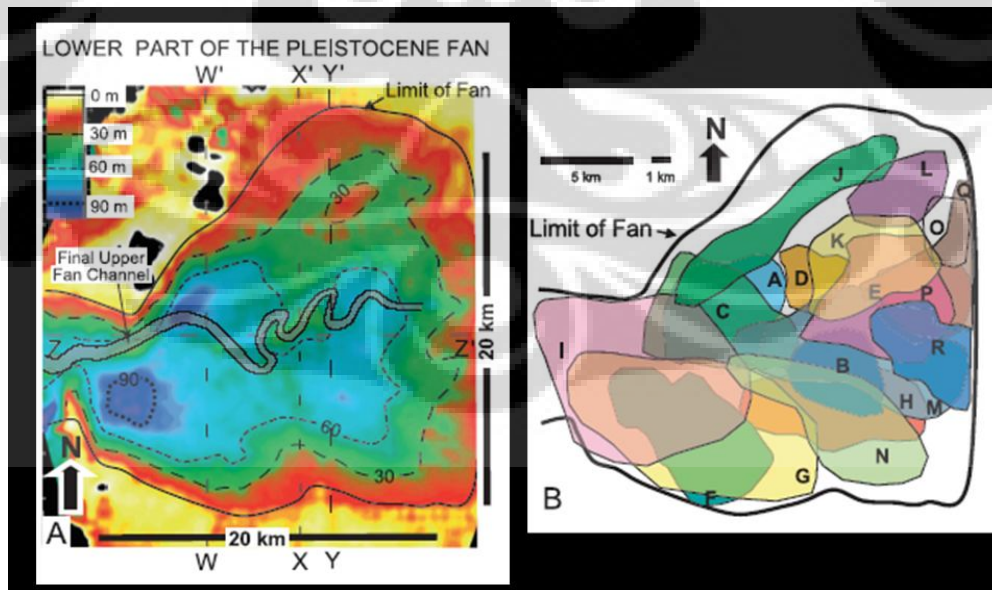


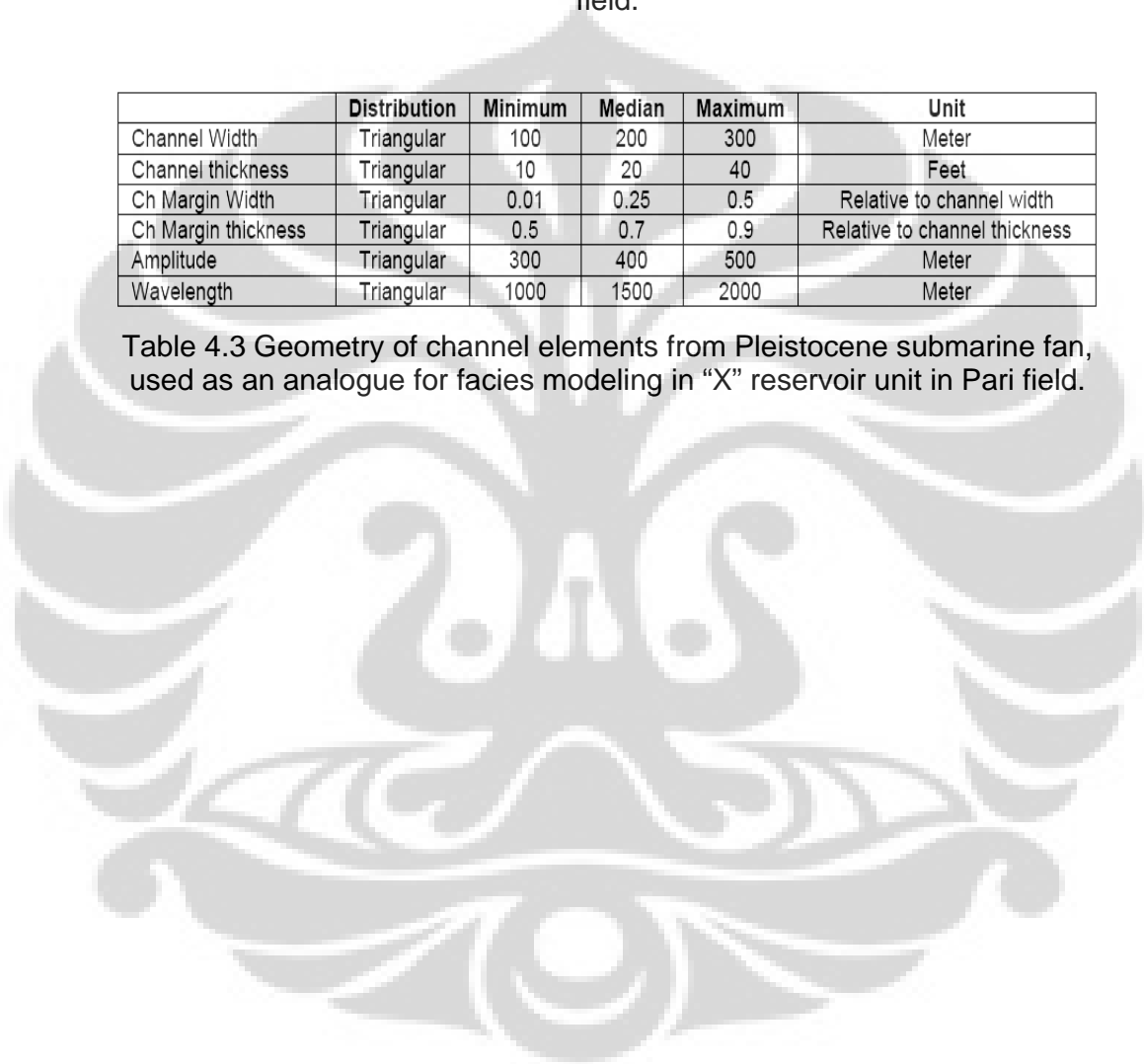
Figure 4.34 Interpreted isochore map from 3D shallow seismic data shows mappable lobes configuration. The boundary area of the submarine fan shows with solid black line (Saller et al., 2004).

	<b>Distribution</b>	<b>Minimum</b>	<b>Median</b>	<b>Maximum</b>	<b>Unit</b>
Minor Width	Triangular	300	700	1300	Meter
Major/minor ratio	Triangular	1	1.5	3	Meter
Thickness	Triangular	5	15	25	Feet

Table 4.2 Geometry of splay lobe elements from Pleistocene submarine fan, used as an analogue for facies modeling in "X" reservoir unit in Pari field.

	<b>Distribution</b>	<b>Minimum</b>	<b>Median</b>	<b>Maximum</b>	<b>Unit</b>
Channel Width	Triangular	100	200	300	Meter
Channel thickness	Triangular	10	20	40	Feet
Ch Margin Width	Triangular	0.01	0.25	0.5	Relative to channel width
Ch Margin thickness	Triangular	0.5	0.7	0.9	Relative to channel thickness
Amplitude	Triangular	300	400	500	Meter
Wavelength	Triangular	1000	1500	2000	Meter

Table 4.3 Geometry of channel elements from Pleistocene submarine fan, used as an analogue for facies modeling in "X" reservoir unit in Pari field.





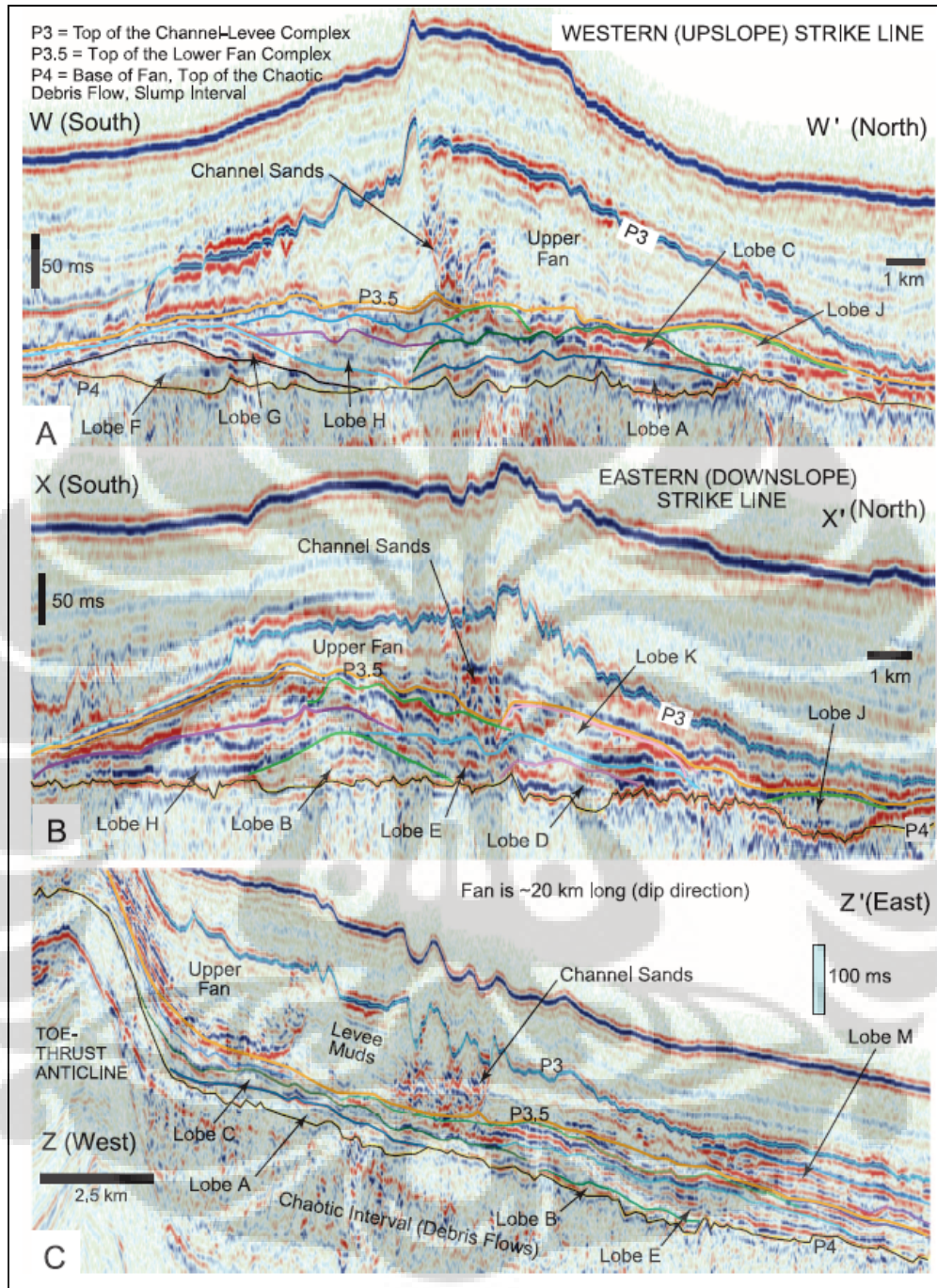


Figure 4.35 Seismic section display along Pleistocene submarine fan with detail interpretation of channel and lobe associated ((Saller et al., 2004).

#### 4.4.5 Pari Field Facies Modeling Result

Based on the Pleistocene submarine fan analogue, the facies modeling for “X” reservoir unit was generated using object based method. The object based modeling assumes that the various facies geometry for “X” reservoir unit is associated with the Pleistocene submarine fan geometries and that their size (width, length and thickness) is random and can be statistically quantified. Based on well data, the facies interpretation is associated with the net to gross ratio. Channel facies associated with high net to gross ratio, medium and low net to gross associated with sheet like splay lobe facies and channel levee. Shale associated with non channel and splay lobe facies that related with hemipelagic deposited.

The submarine fan sediment source interpreted based on regional mapping and has relative N125°E direction of sediment source that feed the submarine fan.

The object based modeling was limited by the outer limit of possible gross sand development of the submarine fan. Outside from the outer limit, it is consider that the sand development to be minor because of the submarine fan thins greatly outside the limit.

The three facies model were generated to provide multiple realizations of facies model. Those are 70% channel and 30% splay lobe (more channels dominated) to represent better reservoir quality with more high net to gross facies and less low net to gross facies, 50% channel and 50% splay lobe (proportional between channel and splay lobe) to represent an equal proportion of high net to gross and low net to gross facies, and 30% channel and 70% splay lobe (more splay lobes dominated) to represent poorer reservoir quality with less high net to gross and more low net to gross facies.

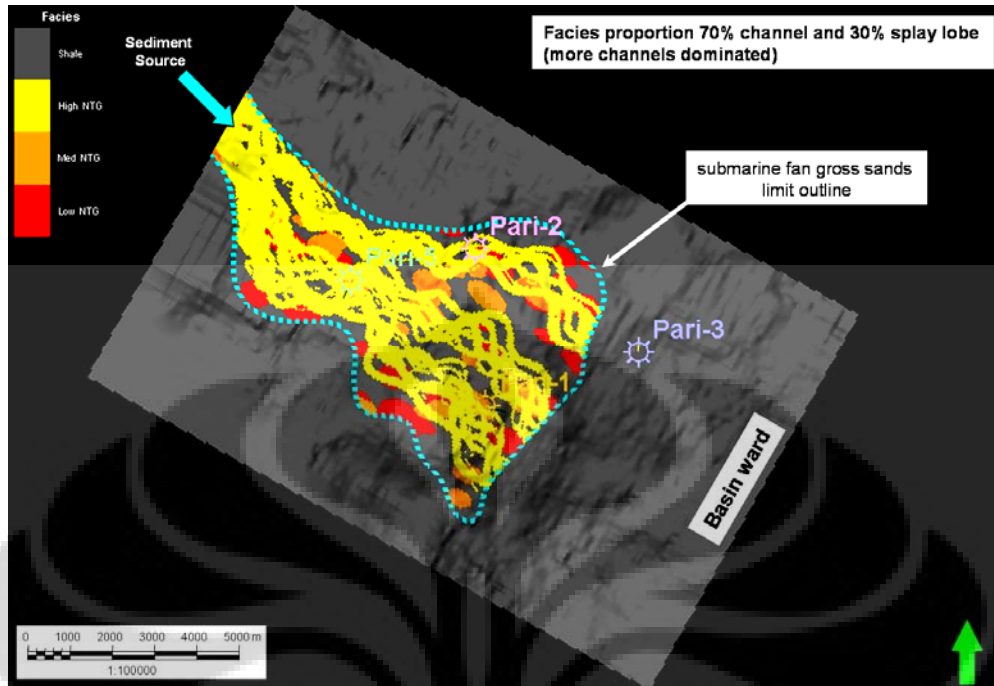


Figure 4.36 Facies realization in the "X" reservoir unit with facies proportion 70% channel and 30% splay lobe (more channels dominated).

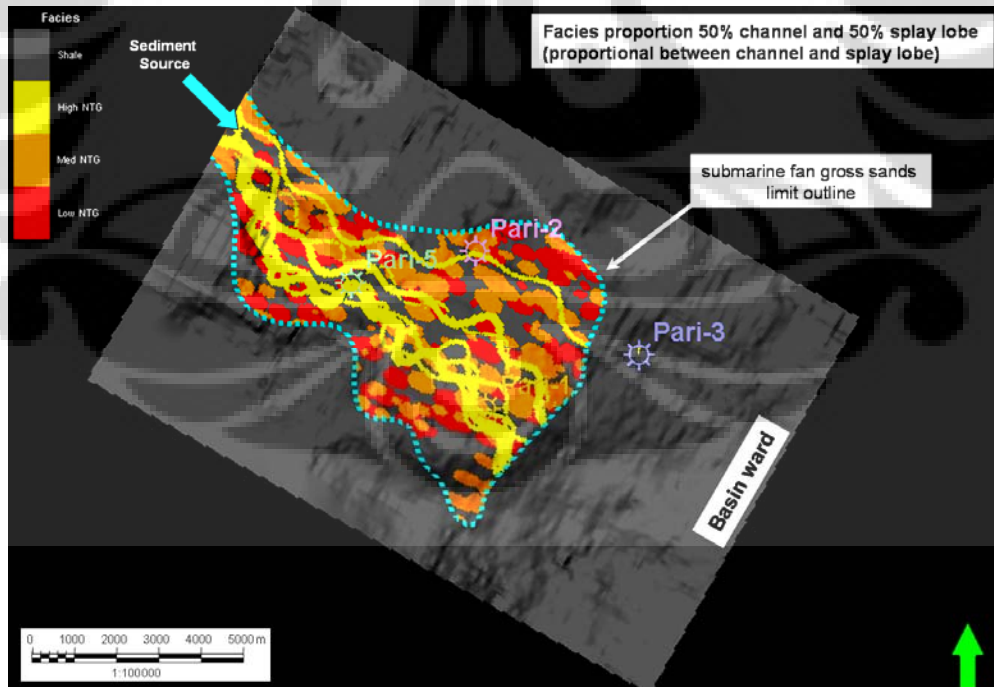


Figure 4.37 Facies realization in the "X" reservoir unit with facies proportion 50% channel and 50% splay lobe (proportional between channel and splay lobe).

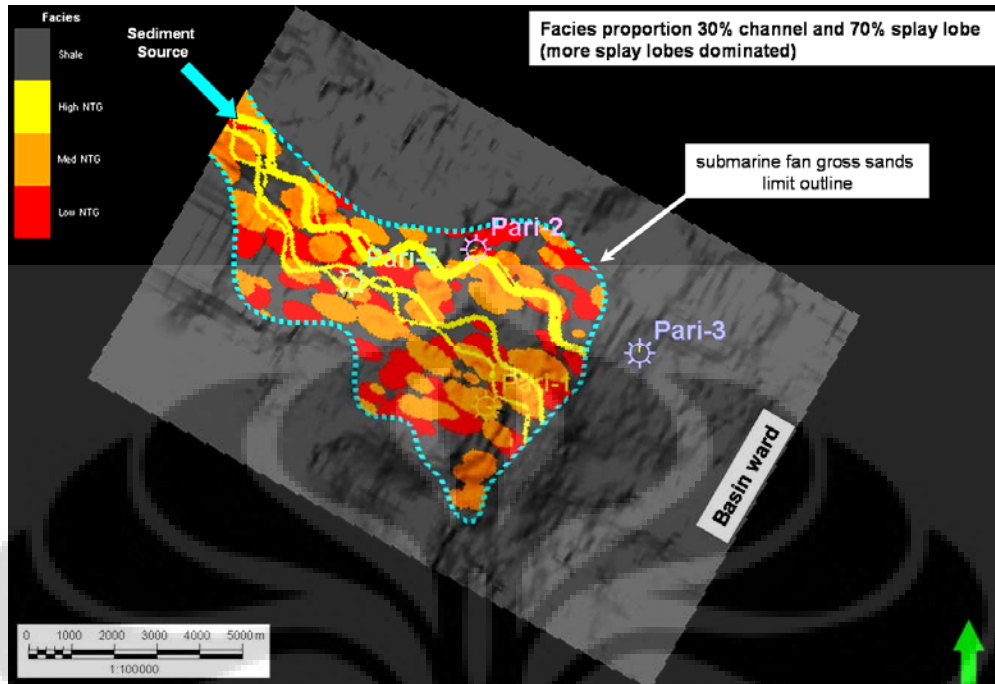


Figure 4.38 Facies realization in the “X” reservoir unit with facies proportion 30% channel and 70% splay lobe (more splay lobes dominated).

## Chapter 5

### Conclusions and Recommendations

#### 5.1 Conclusions

Seismic sequence stratigraphy analysis was performed to identify a chronostratigraphic evolution of submarine fan reservoir in Pari field, Makassar Strait, offshore East Kalimantan. A complete sequence stratigraphy in Pari field was divided into three systems tract: lowstand systems tract (LST), transgressive systems tract (TST) and highstand systems tract (HST). The "X" reservoir unit was deposited during the lowstand systems tract (LST). Based on core data and well log, the reservoir is dominated by few massive thick sandstone, thin interbedded sandstone and shale.

Well data and 3D seismic multiattribute analysis indicated a submarine fan depositional system feature. However, the available 3D seismic data could not image the submarine fan elements feature like channels and splay lobes due to low seismic resolution. A shallow Pleistocene submarine fan located in the northern part of the study area is clearly imaged using 3D seismic data. That Pleistocene submarine fan provides analog dimensions for sub-seismic reservoir elements in the "X" reservoir unit, Pari field. The dimensions of channels and splay lobes within Pleistocene submarine fan were used to define stochastically reservoir elements in Pari field. The Pleistocene submarine fan are approximately the same size as the seismically mapped the "X" reservoir unit. Three facies model were generated to provide multiple realizations of facies model. Those are 70% channel and 30% splay lobe (more channels dominated), 50% channel and 50% splay lobe (proportional between channel and splay lobe), and 30% channel and 70% splay lobe (more splay lobes dominated).

## 5.2 Recommendations for future work

To elaborate many subsurface data (e.g. seismic data, well data), a geostatistics method can be applied to build a 3D reservoir model. Geostatistics attempt to construct a different kind of quantitative model and a more realistic picture of reservoir heterogeneity which do not simply “average” important reservoir variable. The multiple realization models using stochastic method is a reflection of what is not known or a measurement of the “uncertainty” (e.g. facies uncertainty).

A 3D facies modeling using an object based method only reasonable to apply in area which has similarity in geological process and the reservoir dimension can not be resolve using the available datasets. Therefore, a high 3D seismic resolution data is important to capture the reservoir heterogeneity (e.g. facies variation).

## References

1. Dubrule, O., 2003, Geostatistics for Seismic Data Integration in Earth Models, Distinguished Instructor Series No. 6, Soc. of Expl. Geoph. and Eur. Assoc. of Geosc. and Eng.
2. Mamuaya, J.M.B., Biantoro, E. And Gir, R., 1995, The Trace of Sandstone Distribution of Q Layers Using Seismic Amplitude and Inversion: A Case Study in Sangatta Field, East Kalimantan, Proceedings Indonesia Petroleum Association, 24<sup>th</sup> Annual Convention, pp. 425-441.
3. Moss, S. J., Chamber J., 1999, Depositional Modeling and Facies Architecture of Rift and Inversion Episodes in the Kutai Basin, Kalimantan, Indonesia, Proceedings Indonesian Petroleum Association (IPA), IPA99-G-188.
4. Saller, A. H., Noah, J. T., Ruzuar, A. P., Schneider, R., 2004, Linked Lowstand Delta to Basin Floor Fan Deposition, Offshore Indonesia: An analog for Deep-water Reservoirs Systems, AAPG Bulletin V. 88, No. 1, January 2004, page 21-46.
5. Sugiaman, F., Cebastian, A., Werner, K., Saller, A. H., Glenn, D., May, R., 2007, Reservoir Characterization and Modeling of an Upper Miocene Deep-water Fan Reservoir, Gendalo Field, Kutai Basin, Offshore East Kalimantan, Proceedings Indonesian Petroleum Association (IPA), IPA07-G-056.
6. Saller, A. H., Werner, K., Sugiaman, F., Cebastian, A., May, R., Glenn, D., Barker, C., 2008, Characteristics of Pleistocene Deep-water Fan Lobes and Their Application to an Upper Miocene Reservoir Model, Offshore East Kalimantan, Indonesia, AAPG Bulletin, V. 92, No. 7, July 2008, page 919-949.
7. Vail, P. R., 1987, Seismic Stratigraphy Interpretation Procedure, Atlas Seismic Stratigraphy, American Association Petroleum Geology.
8. Weimer, P., Link, M. H., 1990, Seismic Facies and Sedimentary Processes of Submarine Fans and Turbidite Systems, Springer-Verlag.